THE UNIVERSITY OF OKLAHOMA

GRADUATE COLLEGE

PETROLOGY OF THE HENNESSEY SHALE (PERMIAN), WICHITA MOUNTAIN AREA, OKLAHOMA

A THESIS

SUBMITTED TO THE GRADUATE FACULTY

in partial fulfillment of the requirements for the

degree of

MASTER OF SCIENCE

BY

DAVID ALLEN STITH

Norman, Oklahoma

1968

UNIVERSITY OF OKLAHOMA
LIBRARY

Downloaded from SHAREOK. Persistent Handle URL: https://hdl.handle.net/11244/48346

ACKNOWLEDGEMENTS

The author would like to express his gratitude to Dr. Charles J. Mankin for suggesting and directing this thesis; to Dr. Clifford A. Merritt and to Dr. Arthur J. Myers for reading the manuscript and offering valuable suggestions; to Dr. William E. Ham and to Dr. Kenneth S. Johnson for several constructive conversations on the stratigraphy of the area; and to the Oklahoma Geological Survey for furnishing aerial photographs and for partially financing the field work.

Special thanks go to all those graduate students with whom the author had many long and valuable conversations on clay mineralogy and geology as a whole.

Also, appreciation is given to the Phillips Petroleum Company for their financial assistance.

ACKNOWLEDGEMENTS

The author would like to express his gratitude to Dr. Charles J. Mankin for suggesting and directing this thesis; to Dr. Clifford A. Merritt and to Dr. Arthur J. Myers for reading the manuscript and offering valuable suggestions; to Dr. William E. Ham and to Dr. Kenneth S. Johnson for several constructive conversations on the stratigraphy of the area; and to the Oklahoma Geological Survey for furnishing aerial photographs and for partially financing the field work.

Special thanks go to all those graduate students with whom the author had many long and valuable conversations on clay mineralogy and geology as a whole.

Also, appreciation is given to the Phillips Petroleum Company for their financial assistance.

TABLE OF CONTENTS

	Page
ACKNOWLEDGMENTS	iii
LIST OF TABLES	vi
LIST OF ILLUSTRATIONS	vii
INTRODUCTION	1
Location and Description of Area	1
Previous Investigations	3
Methods of Investigation	3
STRATIGRAPHY	6
General Statement	6
Wichita Formation	7
Hennessey Shale	8
El Reno Group	10
MINERALOGY	12
Clays	12
General Statement	12
Illite	12
Chlorite	16
Distribution of the Clays	20
Silicates	36
Carbonates	38
Sulfates	39
Heavy Minerals	41
General Statement	41
Titanium Dioxide Minerals	41
Tourmaline	43
Zircon	46
Garnet	46
Opaque Minerals	47
Important Accessory Minerals	47
Staurolite	47

Page

Chlorite 47
Apatite 48
Trace Accessory Minerals 48
Evaluation of the Heavy Mineral Suite 49

PETROGRAPHY 55

Siltstones 55
Mudstones and Shales 58
Carbonates 59

PROVENANCE AND ENVIRONMENTAL STUDIES 60

Grain Size Analysis 60
Source 73
Environment 76

CONCLUSIONS 78

SELECTED REFERENCES 81

APPENDIX 86

I. Analytical Techniques 86
Sample Preparation 86
Size Fractionation 87
X-ray Diffraction 87
Differential Thermal Analysis 88
Particle Size Distribution Analysis 88
Heavy Mineral Separation 89
Sampling 90

II. Sample Locations 92

III. Measured Sections 94
I. Outcrop A-13 94
II. Outcrops C-1 to C-4 95
III. Outcrops C-9 and C-10 97

IV. Thin-Section Descriptions 100

LIST OF TABLES

Table		Page
1.	Classification of Chlorites	21
2.	Illite Peak/Baseline Intensity Ratios, Line A ...	23
3.	Heavy Mineral Percentages	42
4.	Statistical Parameters of Grain Size	71

LIST OF ILLUSTRATIONS

Figure — Page

1. Outcrop Location Map 2
2. Line A, Chlorite (OOL) Relative Intensity Scatter Diagram 26
3. Line B, Chlorite (OOL) Relative Intensity Scatter Diagram 27
4. Line C, Chlorite (OOL) Relative Intensity Scatter Diagram 28
5. Selected Heavy Mineral Trends 44
6. Cumulative Curve, A-4-a 61
7. Cumulative Curve, A-13-e-1 62
8. Cumulative Curve, A-15-b 63
9. Cumulative Curve, C-1-a-2 64
10. Cumulative Curve, C-3-b 65
11. Cumulative Curve, C-9-c 66
12. Cumulative Curve, C-9-f 67
13. Cumulative Curve, C-9-j 68
14. Cumulative Curve, C-9-m 69
15. Cumulative Curve, C-10-a 70
16. Scatter Diagrams, Statistical Parameters of Grain Size 72

Plate

I. Selected X-ray Diffraction Patterns 31

Page

II. Selected X-ray Diffraction Patterns 33

III. Differential Thermal Analysis Patterns 35

IV. Selected Photomicrographs 52

V. Selected Photomicrographs 54

PETROLOGY OF THE HENNESSEY SHALE (PERMIAN), WICHITA MOUNTAIN AREA, OKLAHOMA

INTRODUCTION

Location and Description of Area

This thesis is a mineralogic and petrographic study of the Hennessey Shale in parts of Greer and Kiowa Counties, Oklahoma. The area extends from Gotebo on the east to Brinkman on the west and includes parts of T. 7 N., Rs. 16 to 20 W.; T. 6 N., Rs. 17 to 22 W.; and T. 5 N., Rs. 19 and 20 W. (figure 1).

The eastern two-thirds of the area is almost flat farmland, in places dissected by steep-sided, intermittent streams. To the west of Lake Altus and the westernmost granite peaks, the topography has a distinct badlands character, particularly along the Elm Fork of the Red River. Numerous siltstone beds, absent to the east, cause the development of minor scarps and benches.

Soil development is good and, in many places, the Hennessey is covered by a thin veneer of residual gravel from the Tertiary terrace deposits. Agriculture is the main industry in the area. Cotton and wheat are the dominant

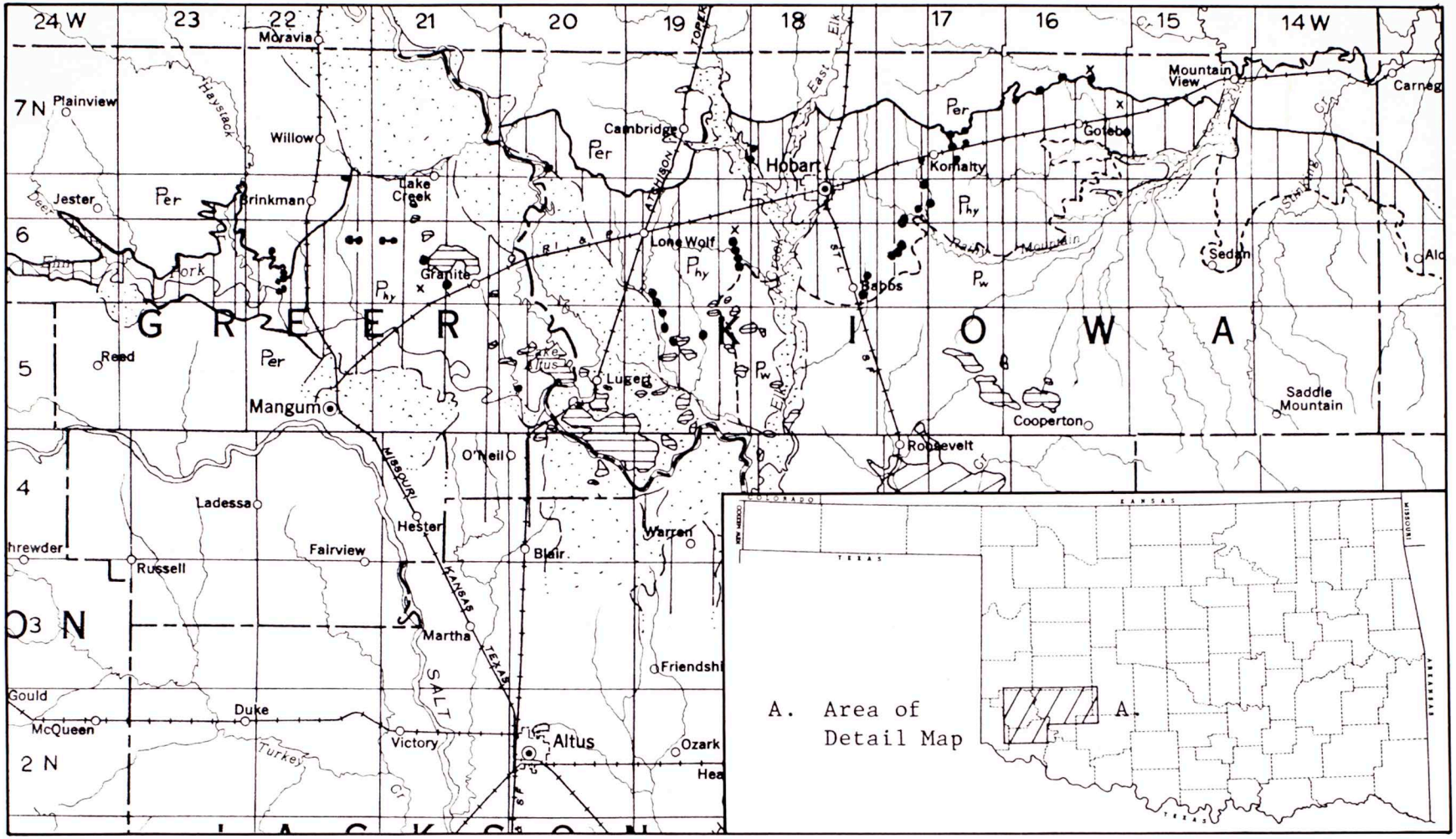

Scale 1:500,000

(Geology adopted from Miser, 1954)

• Outcrops

× Coreholes

Granite

Anorthosite

Alluvium and Terrace Material

Per El Reno Group

Phy Hennessey Shale

Pw Wichita Formation

OUTCROP LOCATION MAP

Figure 1

crops, complementing cattle raising.

The main structural element in the area is the Wichita Mountain uplift. The Hennessey Shale overlies the Wichita Formation; and, in the western one-half of the area, lies unconformably on the granite. Away from the mountains, dips are low, commonly less than 1 degree. Near the mountains, dips from 5 to 15 degrees may be found. To the north, the Hennessey dips into the Anadarko Basin and to the northwest it covers the buried extension of the Wichita Mountains.

Previous Investigations

The only petrographic study to date on the Hennessey north and west of the mountains was done by Dr. R. L. Kerns (University of Oklahoma) who ran clay mineral identifications on several U. S. Army Corps of Engineers core holes which penetrated the Hennessey. These diffractograms were examined by the writer. The remaining work on the Hennessey in this area is limited to field mapping and stratigraphic relationships.

Methods of Investigation

Three general traverses were projected across the Hennessey outcrop: A, from Babbs Switch north to 2 miles north of Gotebo; B, from the vicinity of Dome Mountain north to 3 miles east of Cambridge; and C, from the south end of Lake Altus northwest to Brinkman (figure 1). These traverses were planned to connect with U. S. Army Corps of Engineers

coreholes AL-1, AL-2, Gotebo, and Granite.

Aerial photographs, scale 1:20,000, supplied by the Oklahoma Geological Survey, were then examined for outcrops. Their locations along the three traverses were marked on topographic maps or county road maps and were then field-checked. In the field other outcrops were located. Those outcrops which provided the most continuous sequence of the formation were then described and sampled. Due to the lack of outcrops in line B and the starting point for line C, line A is the only traverse that is fairly continuous from the top to the bottom of the Hennessey. Most of the samples come from outcrops from 1 to 15 feet thick on hillsides and in creek banks. Only three sections were measured; one, approximately 100 feet at the top of the Hennessy in line A; and two sections, 120 and 125 feet in the upper part of the formation in line C. The selection of prospective sample locations in line C was facilitated by detailed field work done by Dr. K. S. Johnson for the as yet unpublished map of Southwestern Oklahoma by Ham and Johnson (Oklahoma Geological Survey).

Mineralogical identification was accomplished by x-ray diffraction using Siemens and North American Phillips (Norelco) equipment and by a petrographic microscope. Additional data from a Norelco x-ray diffractometer equipped with a heating furnace and from a Robert L. Stone Company Model DTA-13M differential thermal analysis unit were used in

identification of the clay mineral suite. Three samples were separated into fractions of 1-4, ½-1, ¼-½, and less than ¼ micron equivalent spherical diameters by the use of a Lourdes Instrument Corporation continuous-flow high-speed centrifuge (Model LCA-1). Particle size distribution was determined using standard laboratory glassware, a set of U. S. Standard Sieve series with a ¼ Ø-unit interval, and a Ro-tap machine. Heavy minerals were separated with tetrabromoethane, centrifuge, and a Frantz Isodynamic Separator.

In all, 120 surface and 10 core samples were analyzed for clay minerals, 5 samples were examined on the diffractometer furnace, 13 samples were x-rayed after HCl treatment, 10 samples were analyzed by sieve, pipette, and heavy mineral separation, and 16 surface and 6 core samples were thin-sectioned.

STRATIGRAPHY

General Statement

The Hennessey Shale is the uppermost member of the Enid Group, underlain by the Wichita Formation, and overlain by the El Reno Group. It is Permian in age and currently assigned to the upper part of the Leonardian Series (Permian Subcommittee, 1960).

In 1905, Gould defined the Enid Formation as all rocks from the base of the Permian to the base of the Blaine. The area surrounding the Wichita Mountains was mapped as "Red Beds of Uncertain Relations" (Gould, 1905, plate I, p. 12). Sawyer (1924) recognized a large basin in western Oklahoma but did not change the designation of the Enid Formation. Gould (1924) proposed the name "Anadarko Basin" and traced the Duncan Sandstone northwestward around the Wichita Mountains. Aurin, Officer, and Gould (1926) elevated the Enid to a group and subdivided it into the Stillwater, Wellington, Garber, Hennessey, Duncan, and Chickasha Formations. This pertained to the northwest and southeast flanks of the Anadarko Basin. The southwest flank of the basin was left as Clear Fork-Wichita, Duncan, and Chickasha

Formations. Sawyer (1929) said the Chickasha was correlative with the Flowerpot Shale, Blaine Formation, and Dog Creek Shale in the western part of the basin. In addition, he said the Garber-Hennessey in Kiowa County was several hundred feet of indistinguishable red shale and thin sandstone. In 1930, Becker classed the Duncan and Chickasha as the El Reno Formation and correlated the Hennessey with the Clear Fork in Texas and the Cedar Hills and upper Salt Plains in Kansas. He gives a thickness for the Hennessey of 600-700 feet, and lists the Garber, Wellington, and Wichita-Albany in descending order below the Hennessey. Schweer (1937) proposed the name El Reno Group for the beds between the Hennessey and the Whitehorse Group. Miser (1954) included the Garber Sandstone, Wellington Formation, and the upper part of the Pontotoc Group under the heading Wichita Formation in the southwest portion of the state.

Wichita Formation

There is little detailed information about the Wichita in this area. Several miles south of the inferred Wichita-Hennessey contact the beds are predominately siltstone, sandstone, and shale. Gypsum and siltstone are more abundant and more of the beds are green than in the Hennessey. As the boundary between the two formations is apparently gradational and exposures in the area of the contact are poor, the contact was taken as shown on the State

Geologic Map (Miser, 1954).

Hennessey Shale

The Hennessey is composed of red and green claystone, mudstone, and thin-bedded siltstone with some gypsum veins and seams. However, in the Wichita Mountain area the siltstone content is variable. East of Lake Altus, the formation is mainly shale and claystone, with a few thin siltstone beds and silty shale layers. The uppermost 10 to 40 feet is normally yellow to tan shale and silty shale commonly interbedded with thin limonite zones and concretions. The contact with the overlying Duncan is unconformable. In addition to the indications of an oxidized zone at the top of the Hennessey numerous channels are cut at the base of the Duncan. Interfingering of the basal Duncan siltstones and the upper Hennessey shale indicates the contact is not a constant time-stratigraphic horizon.

In the western portion of the area, five siltstone beds are prominent. Dr. K. S. Johnson (personal communication, 1966) has determined that the uppermost bed is approximately 50 feet below the stratigraphic level of the basal Duncan. This bed has been mapped as the Duncan in the region west of Lake Altus. The five siltstones are from 1 to 10-15 feet thick and are continuous. They can be traced for miles along the Elm Fork of the Red River. The total thickness of these beds and the intervening shale is 100-120 feet. For

mapping purposes, Johnson designated these beds, in ascending order, "W", "X", "Y", "Z", and the "Brinkman Bed". This nomenclature is also used by the writer. The siltstones are light gray to gray-green, micaceous, slightly friable, and commonly laminated. Ripple marks are seen in places as well as minor channels. There is no major difference in the composition of the shale in the two regions. Some scattered grains of quartz and feldspar, up to 2 mm in size, are found both in the shale and in the siltstone. These are almost completely limited to the western portion of the area.

Most Hennessey exposures show only minor, if any, amounts of arkosic material. In a few localities the Hennessey is preserved where it directly overlies the granite. This near-shore facies is composed of maroon, orange, and black sandstone and shale. Some conglomeratic layers are present. No exposures with appreciable arkosic material were found more than a mile from granite outcrops and most were within half a mile.

Some of the green color in the shale is directly associated with bedding but most of it is not. The red shale contains few to abundant green reduction spots 0.1 mm to 25 mm or more in diameter. Some large-scale, red-green contacts exist which seem to be bedding, but which, on close examination, are inclined at least 20 degrees to bedding. Also, many outcrops show irregular streaks of green coloration, cutting across bedding at all angles from horizontal

to near vertical. These normally can be seen to follow fractures or joints in the shale. Although many of the silty layers are red, almost all of the siltstones are light gray to gray-green.

Gypsum is present throughout the section. Selenite and satin spar veins and seams are found in a few outcrops and are numerous in the cores. Many outcrops are covered with small selenite crystals, probably formed by weathering. Most of the gypsum seems to be secondary, rather than recrystallized from depositional anhydrite or gypsum. Malachite-staining is observed in several outcrops in the upper, oxidized portion of the Hennessey. Trace amounts of barite are present as rounded concretions, vein material, and granular cement.

El Reno Group

The lower two units in the El Reno Group are the Duncan Sandstone and the Flowerpot Shale. The Duncan is similar to the underlying Hennessey and the overlying Flowerpot. It differs from both formations in two aspects: first, the Duncan contains more green to tan shale than either of the other two formations and second, the siltstone and sandstone tend to be light to medium gray, compact or cross-bedded, resistant bench-formers in the Duncan as opposed to the laminated, friable Hennessey siltstone and lack of siltstone in the Flowerpot.

In the type-section, the Duncan consists mainly of sandstone, minor siltstone, and some interbedded shale (Self, 1966). To the northwest, the shale content increases and the Duncan grades into the Flowerpot. In sec. 24, T. 7 N., R. 21 W., Scott (1955) gives a Duncan thickness of 28 feet including a total of 10 feet of siltstone and sandstone. West of the alluvium deposits along the North Fork of the Red River, the Duncan is no longer recognizable and the Hennessey grades directly into the lithologically similar Flowerpot. Due to the lack of resistant beds, the interval between the Hennessey "Brinkman Bed" and the upper part of the Flowerpot forms low, rolling topography with few exposures. Because of this and the similarity of the Hennessey and Flowerpot, the contact between these two formations in the thesis area cannot be found.

MINERALOGY

Clays

General Statement

Clay mineralogy of the Hennessey is uniform throughout the area. Illite is present in all samples and chlorite is found in over 90 percent of them. Also present in minor amounts are alteration products of both illite and chlorite.

Illite and chlorite are phyllosilicates. Illite is the term for the clay-size varieties of mica whereas chlorites are not broken down on a size basis. Illite is a 3-layer clay mineral based on the muscovite structure and the chlorites are 4-layer structures, combining an aluminum or magnesium hydroxide layer (gibbsite or brucite) with the standard 3-layer mica structure.

Illite

Muscovite is a 3-layer phyllosilicate based on the pyrophyllite structure (see Grim, 1953, p. 66, for details of the muscovite structure). Illite differs from well-crystallized muscovite in several ways. There is less substitution of aluminum for silicon in the tetrahedral layer

resulting in a decrease in the charge deficiency and amount of interlayer potassium. Some of the potassium ions, which balance the charge deficiency, may be replaced by aluminum hydroxide complexes, calcium, or hydronium ions. Minor substitution of iron and magnesium may take place in the octahedral layers. Also, the degree of crystallinity of illite is lower than that of muscovite.

In the Hennessey, illite is present in all samples. Size fractionation indicates it occurs in all sizes down through less than 1/8 micron. Identification of illite is made from x-ray diffraction peaks at 10, 5, 4.5, and 3.3 Å on an oriented slide. The sharpness of the peaks ranges from good to poor, depending mainly on crystal size. Sample C-3-b, for example, shows a peak-height to ½ peak-height-width ratio of 33 for the 1-4 micron fraction. This decreases to 10 for the ½-1, ¼-½, and less than ¼ micron fractions and to 4.3 for the less than 1/8 micron fraction (plate I). Although much of this broadening is due to decreasing particle size, there are two other causes for some of it. Many samples show a 10 Å peak that is broadened on the low-angle side. Solvation with ethylene glycol merely sharpens this reflection. There is no shift in the d-spacings at 10 Å or 3.3 Å nor is there any subsidiary peak developed between 10 and 11 Å. These are the so-called "degraded" illites (Grim, 1951). Potassium has been stripped from some interlayer positions and replaced by water. The

increased sharpness after solvation results from extraction of water from the interlayer region by ethylene glycol. A few other samples, such as A-7-a (plate II), show a shift to lower and higher d-spacings for the 10 Å and 3.3 Å peaks, respectively, on solvation. In addition, a secondary peak or shoulder is developed between 10 and 12 Å. This is interpreted as an illite-montmorillonite mixed-layer sequence with 10 to 20 percent montmorillonite (Weaver, 1956). However, treatment of both types of clay with a 1N KOH solution for 10 hours shows that the mixed-layer material is also derived from the illite and is merely a highly "degraded" form of illite in which some cation besides water has replaced the potassium (Weaver, 1958a). The treated clays show a more symmetrical peak at 10 Å than the untreated samples and give no indication of sharpening or expansion on solvation (plate II).

As the coarser clay fractions contain appreciable amounts of quartz, feldspar, dolomite, and chlorite, it is difficult to determine the type of illite present. Random-oriented patterns of all fractions show (060) spacings in the range of 1.50-1.51 Å which is indicative of a dioctahedral structure. No tendency toward a trioctahedral structure is shown even by the less than ¼ micron size. Polymorph determination is difficult because of contamination in the coarser fractions and the effect of particle size in the finer fractions. The dominant mica polymorph present is

probably 2M with a minor amount of 1M (plate I). Polymorph determination is made by comparison of the powder data with that of Yoder and Eugster (1955).

DTA patterns of the illite show a minor to pronounced endotherm at about 80°C. This corresponds to the loss of interlayer water; there is a rough correlation between the broadening of the 10 Å peak and the size of the low temperature endotherm. A second endotherm begins between 300° and 400°C with a maximum at about 520°-540°C. This is correlated with dehydroxylization of the lattice (Grim, 1953). A third and minor endotherm between 850° and 880°C correlates with the beginning of the final destruction of the illite structure as shown by diffractometer furnace treatment. This endotherm probably represents a structural reorganization rather than a loss of material (Grim, 1953).

DTA patterns of two limonite zones from the upper Hennessey show a minor endotherm between 200° and 300°C (plate III). There is no chlorite in these samples but a material which expands to as much as 17 Å is present. Potassium treatment, which collapses this peak to 10 Å and prevents re-expansion on solvation, and the 200° to 300°C endotherm indicate that the material is a montmorillonoid with a high tetrahedral charge deficiency being formed from the alteration of illite. The term collapse refers to a reduction in spacing in the "c" axis direction.

Chlorite

Trioctahedral chlorites are composed of alternating talc and brucite structures. The corresponding dioctahedral structure would be pyrophyllite and gibbsite. The many varieties of chlorite arise from isomorphous substitution in both structures. The most common substitutions are iron and aluminum for magnesium both in the octahedral layer of the talc structure and in the brucite structure and aluminum for silicon in the tetrahedral layers of the talc structure (Brown, 1961).

Chlorite is present in almost all samples of the Hennessey. Near-shore facies and the limonite zones in the upper part of the formation are the only two normally chlorite-free lithologies. These two facies will be discussed under Distribution of the Clays. Where present, the chlorite is normally found in all sizes, but several samples give indications of chlorite only in the coarser fractions. Chlorite identification is made by reflections near 14.2, 7.1, 4.75, and 3.5 Å on an oriented slide. Kaolinite, which can overlap the 7 Å and 3.5 Å peaks, has a peak at 2.383 Å and is insoluble in warm, dilute HCl. The structure factor for the chlorite peak in the vicinity of 2.38 Å is such that it is seldom detected. Also, chlorite is soluble in HCl. No peak was detected at 2.38 Å for any of the samples. In addition, 13 samples were treated for 8-12 hours with warm HCl. All four chlorite peaks vanished in most samples, and

in those that still retained the 14 Å peak and suborders, the 7 and 3.5 Å peaks were not enhanced.

Further evidence of chlorite is the fact that on ethylene glycol solvation the peaks in question do not expand. Likewise, treatment with 1N KOH for 10 hours had no effect on the 14 Å peak. Diffractometer furnace patterns indicate that the chlorite in the Hennessey does not behave like normal, coarser chlorites on heating. All orders except the 14 Å disappear by 450° to 500°C. The 14 Å peak, however, disappears in the range of 600°-700°C but does so without noticeable increase in intensity as is normally observed. The low temperature of destruction is attributed to poor crystallinity (Brown, 1961). Further evidence of poor crystallinity is shown by the DTA patterns. Only two patterns show minor endotherms at 620°-640°C that can be attributed to chlorite (plate III). The absence of chlorite endotherms is also partly due to less chlorite than illite in all samples.

Several gross clay samples show minor amounts of material that expand slightly on solvation. For some samples this is a discrete peak about 5.5 degrees 2θ but normally is only a shoulder about 6 degrees on the main chlorite peak. The previously mentioned size-fractioned sample, C-3-b, is one of these. The 1-4 micron fraction shows only minor expansion to 17.16 and 15.78 Å, the ½-1 micron fraction shows one-half the 14 Å peak expanding to 17.33, 16.67, and

and 16.07 Å, the ¼-½ micron fraction has over one-half the peak expanding to 17.14 and 15.52 Å, and the less than ¼ micron fraction has most of the 14 Å peak expanding to 16.07 and 15.5 Å. All three of the finer fractions also show a separation from the 7 Å peak. Samples of the finer three fractions sedimented on ceramic plates show rehydration to 14 Å when heated to 500°C. By 550°C there is only partial rehydration to 12.65-14.03 Å and by 800°C there is no rehydration. The rehydration occurs on cooling to room temperature.

DTA patterns of C-3-b show: (1-4 microns) weak illite pattern modified by dolomite; (½-1 micron) illite pattern with possible minor chlorite endotherm at 620°-640°C; (¼-½ and less than ¼ micron) illite pattern plus a strong endotherm at 570°C and an S-shaped endotherm-exotherm from 800° to 900°C (plate III).

Furnace diffractograms of the ¼-½ micron fraction of C-3-b show a partial collapse to 12.61 Å by 150°C in addition to the 14 Å peak. The 12.6 Å peak disappears on further heating and the 14 Å peak is lost at about 600°C. The less than ¼ micron fraction behaves quite differently in the furnace. The 14 Å peak shows a gradual loss in intensity and collapses to a broad peak from 12.6 Å to 14 Å by 250°C at which point it collapses completely. The 10 Å peak collapses at the same time from 10.16 to 10.05 Å, and an intense superorder appears at 23.25 Å. The superorder stays

at approximately the same position until 600°C where it disappears. The sum of all these data indicates that in the finer fractions the chlorite is being altered to a vermiculite-like material which is randomly interlayered with the unaltered chlorite. This is shown by the numerous peaks obtained on solvation and is best illustrated in the finest fraction where the long-range spacing, 23.25 Å, is interpreted as mixed-layer chlorite-vermiculite, 14.20 Å + 9.02 Å (the vermiculite in a collapsed state due to heating). Further suggestion of the interlayering is the fact that the superorder disappears at 600°C, the same temperature that the chlorite in the coarser fractions disappears. Proof that the material is being altered from chlorite, not illite, is shown by a trioctahedral (060) spacing (1.535 Å) and the fact that potassium saturation does not affect the expansion on glycol solvation.

A classification of several of the chlorites was attempted using the classification of Hey (1954) and obtaining the necessary data by the diffraction method of Shirozu (1958). The trioctahedral nature of the chlorites is shown by (020) reflections at 4.58-4.63 Å and (060) reflections at 1.535-1.556 Å. Because the chlorite is mixed with illite, quartz, and dolomite, it is impossible to determine the nature of the coarser fractions in most cases. Four samples were classified: A-19-d, less than four microns; C-3-b, 37-62.5, 1-4, and ½-1 micron fractions. Hey's classifica-

tion is based on the amount of silicon in the tetrahedral layer and the ratio of total iron to iron plus magnesium. It is further broken down into the orthochlorites and the oxidized chlorites. Although the coarse sample from C-3-b (heavy mineral separation) has rather low intensity (001) and (003) peaks it is regarded as an orthochlorite. The (060) reflection for sample A-19-d is also doubtful because a minor amount of quartz is present in the sample. Assuming the formula $(Mg_{6-x-y}Fe^{2+}_{y}Al_{x})(Si_{4-x}Al_{x})O_{10}(OH)_{8}$ (Brown, 1961), the chlorites can be classified by Hey's method. Shirozu (1958) verified and refined relationships between y and the "b" parameter and between x and d(001) as taken from x-ray diffraction data. These relationships are given in equation form by Brown (1961): $b=9.21+0.037y$, $d(001)=14.55-0.29x$. For the four samples classified, the "b" parameter was obtained from the (060) peak on the powder pattern and the (001) d-spacing obtained by averaging d(001) derived from the (003), (004), and (005) peaks on a sedimented pattern (Martin, 1955). The critical d-spacings, derived data, and classifications are shown in table 1.

Distribution of the Clays

Three regional trends in the clay minerals were observed in the thesis area, one vertically, one lithologically, and one laterally. A chlorite-illite index (Everett, 1962) which is the ratio of the intensity of the 7 Å chlorite

Sample	size in microns	d(001)*	"b"	x	y	Si	R
C-3-b	37-62.5	14.138	9.288	1.42	2.11	2.58	0.46
C-3-b	1-4	14.165	9.210	1.33	0	2.67	0
C-3-b	½-1	14.166	9.222	1.32	0.32	2.68	0.07
A-19-d	<3.6	14.220	9.336	1.14	3.40	2.86	0.70

	C-3-b						A-19-d	
	37-62.5		1-4		½-1		<3.6	
hkl	d	I	d	I	d	I	d	I
001	14.19	1.8	14.23	7.2	14.03	10.0	14.26	7.7
002	7.08	10.0	7.08	10.0	7.115	5.9	7.092	10.0
003	4.713	2.8	4.74	2.9	4.77	4.9	4.745	2.6
004	3.353	6.7	3.53	6.5	3.512	5.7	3.534	5.8
005	2.827	1.0	2.831	1.6	2.858	2.6	2.858	2.3
060	1.548	w	1.535	m	1.537	m	1.556	m
Name	Ripidolite		Sheridanite				Brunsvigite	

* d(001) averaged from 003, 004, and 005.

CLASSIFICATION OF CHLORITES

Table 1

peak to twice the intensity of the 5 Å illite peak was computed for all of line A and for the part of line C where certain beds were sampled in two different areas. No correlation was found in either line between the ratio and sediment color, lithology, or stratigraphic position. An indication appeared, however, that the ratio depended mostly on the crystallinity of the clay and the degree of preferred orientation of the slide; these two factors affected the height of the chlorite peak more than the illite peak. No further work was done on this ratio.

Numerous samples in line A show an elevated baseline in the low angle region (plate II). This is more pronounced in the lower part of the section and is quite similar to samples of the Wichita Formation. It is partly due to the degraded nature of the illite and partly to the mixture of illite and chlorite. In order to check the vertical change of this phenomenon, the ratio between the intensity of the 10 Å illite peak and the intensity of the low point of the baseline between this peak and the 14 Å chlorite peak was computed. The intensities were taken as the height above a baseline projected from the baseline on the high-angle side of the illite peak. The results of these computations are shown in table 2. There are two noticeable increases in both the magnitude of the ratio and in the variation of it, one between samples 8-a and 8-b and one between 10-a and 10-b-1. The first eight outcrops approximately parallel the Hennessey-

Sample	Ratio	Sample	Ratio	Sample	Ratio
A-1-a	1.16	A-9-b-2	2.36	A-13-m-2	5.40
A-1-b	1.12	A-9-c	2.82	A-13-o-3	6.04
A-2-a	1.52	A-10-a	1.93	A-13-p-2	5.76
A-2-b	1.46	A-10-b-1	4.78	A-13-p-3	6.76
A-3-a	2.53	A-10-b-2	5.48	A-13-p-4	5.91
A-5-a	1.78	A-10-c	5.79	A-13-p-7	4.14
A-6-a	1.23	A-11-a	6.62	A-14-a	2.42
A-6-b	1.61	A-11-b	5.34	A-15-c	3.93
A-6-d	1.20	A-11-c	2.10	A-15-d	5.92
A-6-h	5.37	A-11-d	2.54	A-15-e	3.90
A-7-a	1.57	A-11-e	6.23	A-15-f	3.48
A-7-b	1.67	A-11-f	8.45	A-17-a	4.25
A-7-c	1.16	A-12-a	4.36	A-17-b	3.49
A-8-a	1.32	A-12-b	4.16	A-17-c	4.50
A-8-b	2.78	A-13-c	5.35	A-18-a	4.28
A-8-c	4.79	A-13-e-2	2.42	A-19-a	3.63
A-8-d	2.35	A-13-i	7.82	A-19-b	5.71
A-9-a	3.94	A-13-1-1	7.70	A-22-b	3.86
A-9-b-1	3.31	A-13-k	9.40		

LINE A, ILLITE 10 Å REFLECTION

PEAK TO PRE-PEAK-BASELINE INTENSITY RATIO

Table 2

Wichita contact (figure 1). The affinities these patterns show to the Wichita and the abrupt change in the ratio as the traverse swings away from the inferred contact (Miser, 1954) could mean that although the contact is not exposed in this area and is gradational, it can be distinguished on the basis of clay mineral zonation. Reasons for the second increase are less clear as the outcrops are scattered and there is no stratigraphic control.

Chlorite is absent in two types of samples. First, in the limonite zones of the upper Hennessey, chlorite is absent, natrojarosite is found, and even the illite has been altered to montmorillonite and illite-montmorillonite mixed-layer material. This is due to leaching of the clays on an unconformity between the Hennessey and the Duncan. Natrojarosite is a low temperature-pressure mineral (Brophy and Sheridan, 1965). Gypsum present in the section provided the sulfate for its formation, the iron was derived from the destruction of chlorite, and both potassium and sodium could have been derived by leaching the already degraded illite.

Second, most of the samples from outcrops directly overlying granite are either devoid of chlorite or have chlorite only in fractions of 3-4 microns and coarser. It seems probable that considerable concentration of groundwater drainage has taken place at the Hennessey-granite interface (C. R. Nichols, personal communication, 1967). This would

accelerate alteration of the clays and would probably destroy the finer-grained material first. The illite in these samples is normally more altered than in the rest of the samples.

The intensities of the first four chlorite peaks on sedimented patterns show quite a variation between different samples: (001) weak to strong, (002) medium to strong, (003) absent to medium, and (004) weak to strong. To determine if there was any pattern discernable, plots were made of the intensities from most of the gross clay patterns. The data plotted were the ratio of the intensities of three peaks, (001) versus (002) and (001) versus (003). As the resulting graph was one elongate scattering of points, each line was replotted on a separate graph. From these graphs it is obvious that there is a progressive increase in the (001) intensity in relation to both the (002) and (003) orders in the western portion of the area (figures 2-4). Averages of the two ratios were computed for each of the three lines and plotted. They fall on a line which is in fair agreement with the axis of each scatter diagram. Not only does the (001) peak increase in intensity, the increase is the same in relation to both the (002) and (003) peaks. This is shown by the percentage change in average ratios: line A to line B, I_1/I_3 up 10.6, I_1/I_2 up 12.1; line B to line C, I_1/I_3 up 23.7, I_1/I_2 up 25.9.

Structure factors of chlorite are such that only the odd-order reflections are affected by changes in the brucite

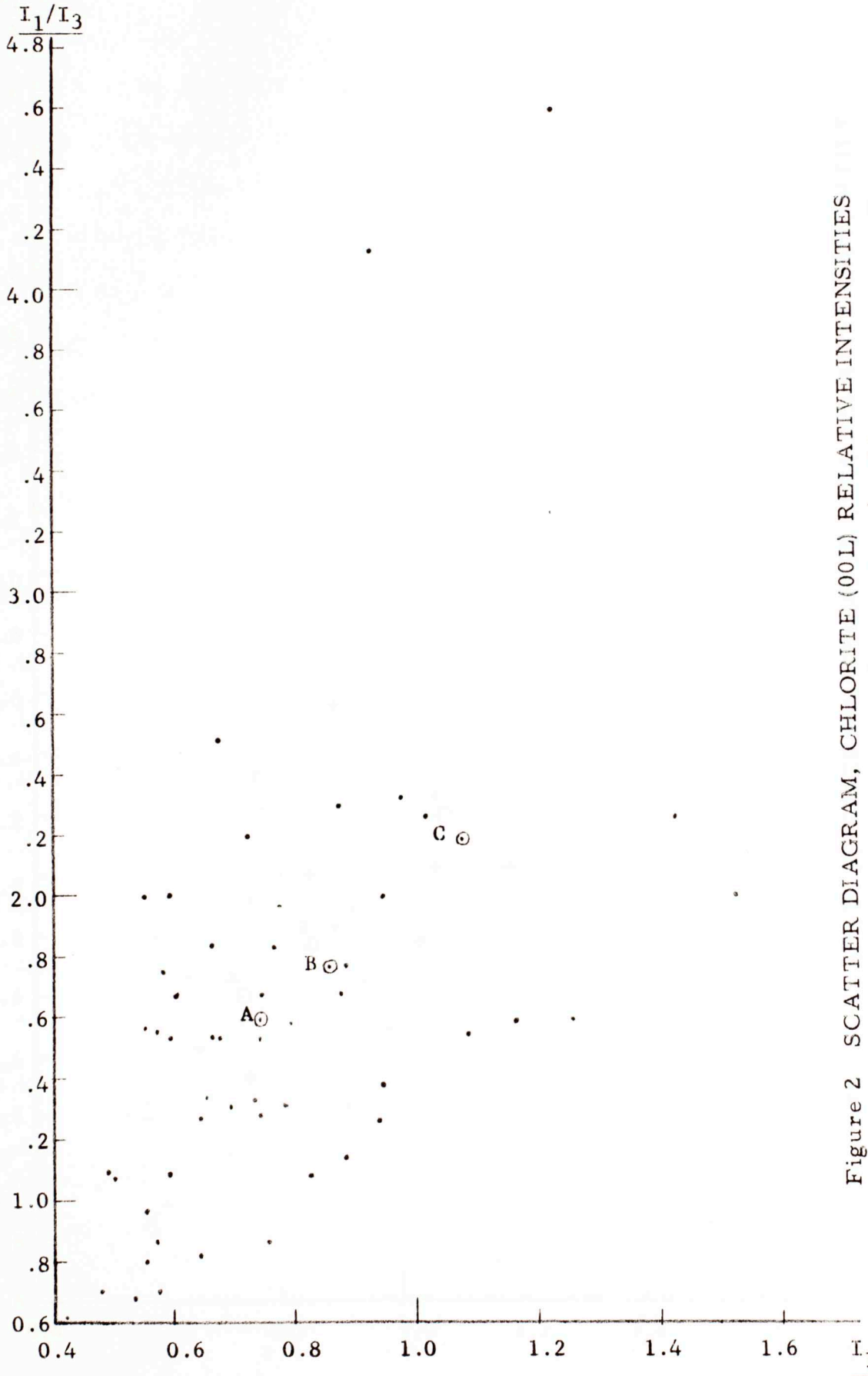

Figure 2 SCATTER DIAGRAM, CHLORITE (00L) RELATIVE INTENSITIES
Line A - •
Line Averages - ⊙A, etc.

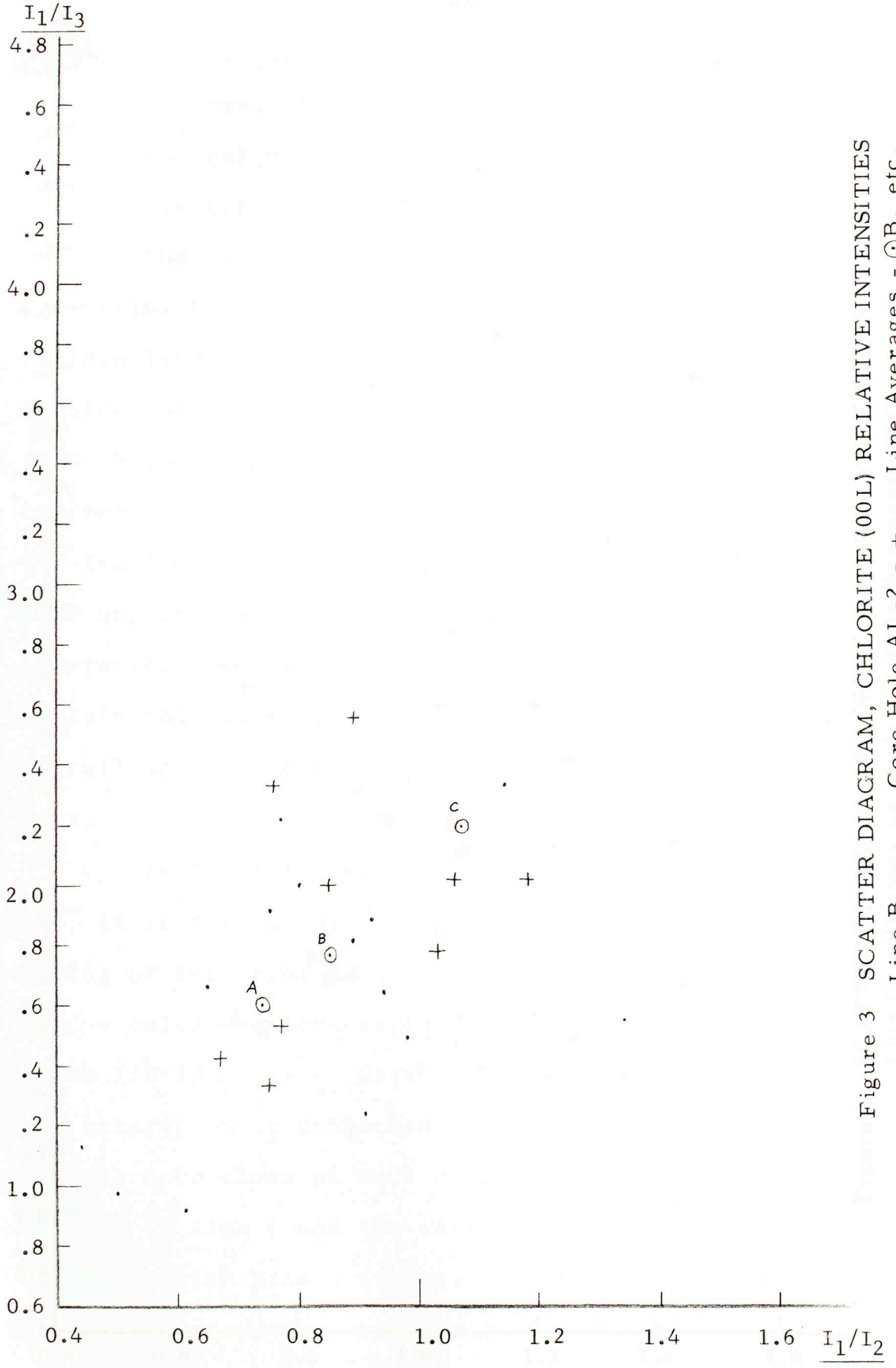

Figure 3 SCATTER DIAGRAM, CHLORITE (00L) RELATIVE INTENSITIES
Line B - • Core Hole AL-2 - + Line Averages - ⊙B, etc.

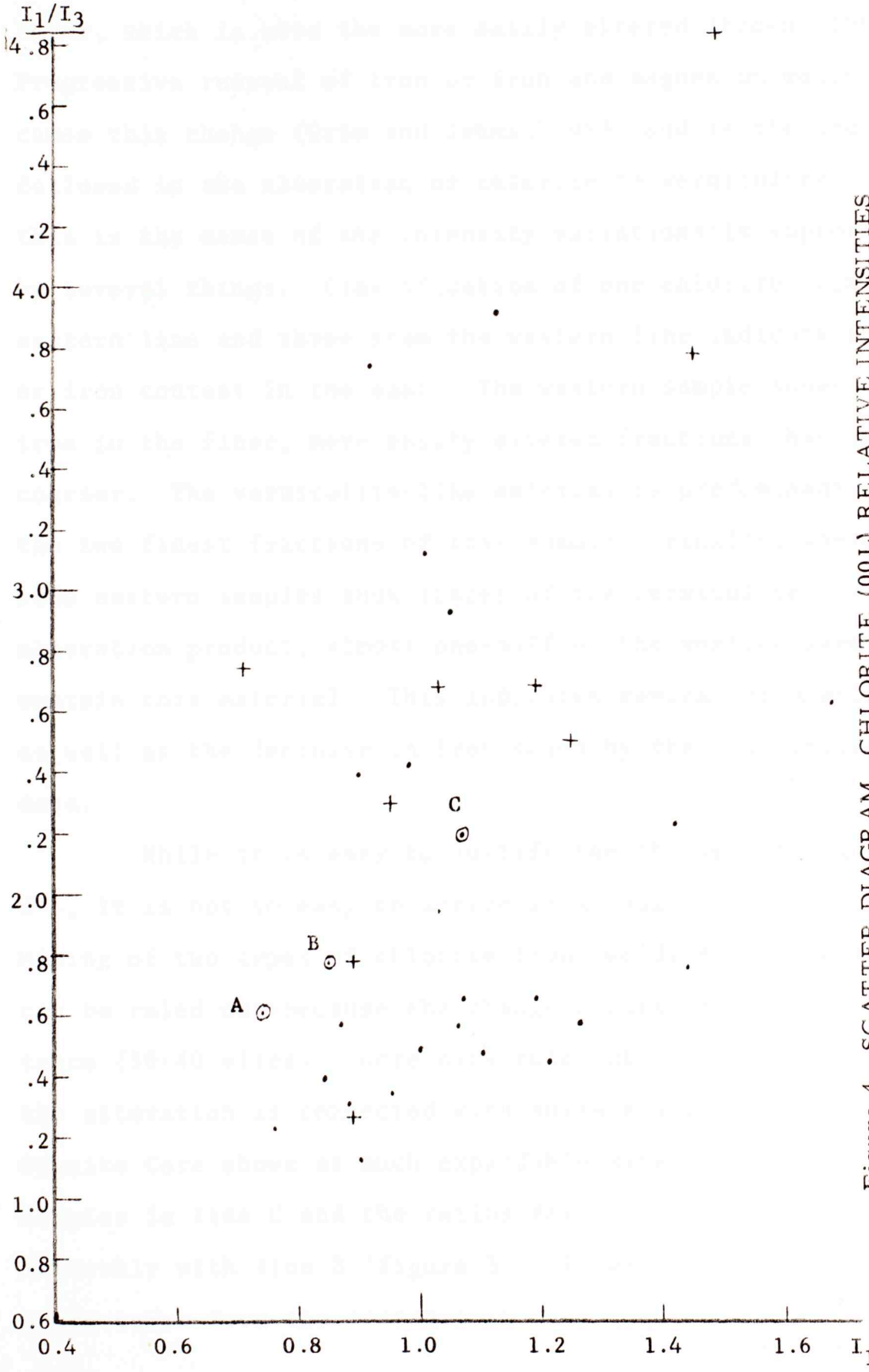

Figure 4 SCATTER DIAGRAM, CHLORITE (00L) RELATIVE INTENSITIES
Line C - siltstone -+ shale -· Line Averages - ⊙C, etc.

layer, which is also the more easily altered (Brown, 1961). Progressive removal of iron or iron and magnesium would cause this change (Grim and Johns, 1953) and is the process followed in the alteration of chlorite to vermiculite. That this is the cause of the intensity variations is supported by several things. Classification of one chlorite from the eastern line and three from the western line indicate a higher iron content in the east. The western sample shows less iron in the finer, more easily altered fractions than in the coarser. The vermiculite-like material is predominant in the two finest fractions of this sample. Finally, whereas some eastern samples show traces of the vermiculite-like alteration product, almost one-half of the western samples contain this material. This indicates removal of magnesium as well as the decrease in iron shown by the classification data.

While it is easy to justify the changes in figures 2-4, it is not so easy to arrive at a cause for the changes. Mixing of two types of chlorite from two different sources can be ruled out because the change occurs in a short distance (30-40 miles). Core data rule out the possibility that the alteration is connected with surface weathering as the Granite Core shows as much expandable material as surface samples in line C and the ratios for the AL-2 Core compare favorably with line B (figure 3). Probably the best explanation comes from the increase in silt in the western area

Plate I

SELECTED X-RAY DIFFRACTION PATTERNS

A.	A-13-p-5	Natrojarosite, powder pattern
B.	C-3-b	$< \frac{1}{4}$ micron, sedimented, solvated; Illite, Chlorite/Vermiculite
C.	C-3-b	$< \frac{1}{4}$ micron, sedimented, humidified; Illite Chlorite/Vermiculite
D.	C-3-b	1-4 microns, sedimented, solvated; Illite Chlorite, Chlorite/Vermiculite, Quartz, Feldspar, Dolomite
E.	C-3-b	1-4 microns, sedimented, humidified; Illite, Chlorite, Chlorite/Vermiculite, Quartz, Feldspar, Dolomite
F.	A-13-p-5	$\frac{1}{4}$-$\frac{1}{2}$ micron, K^+ treated, powder pattern; Illite (2M polymorph)

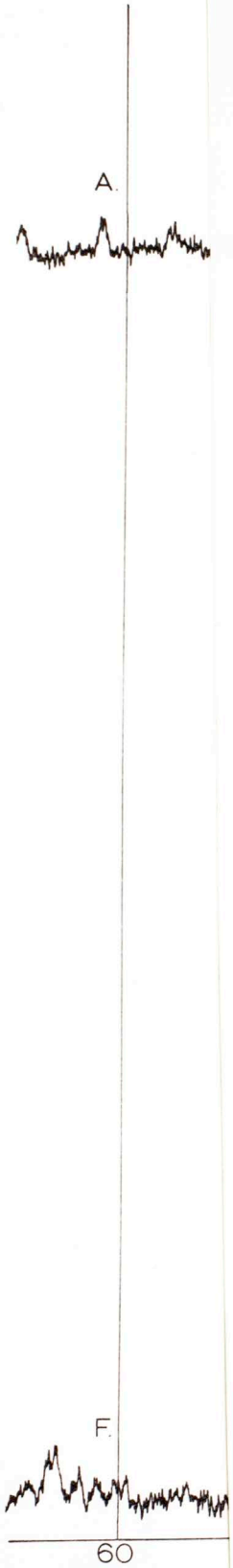
A.
F.
60

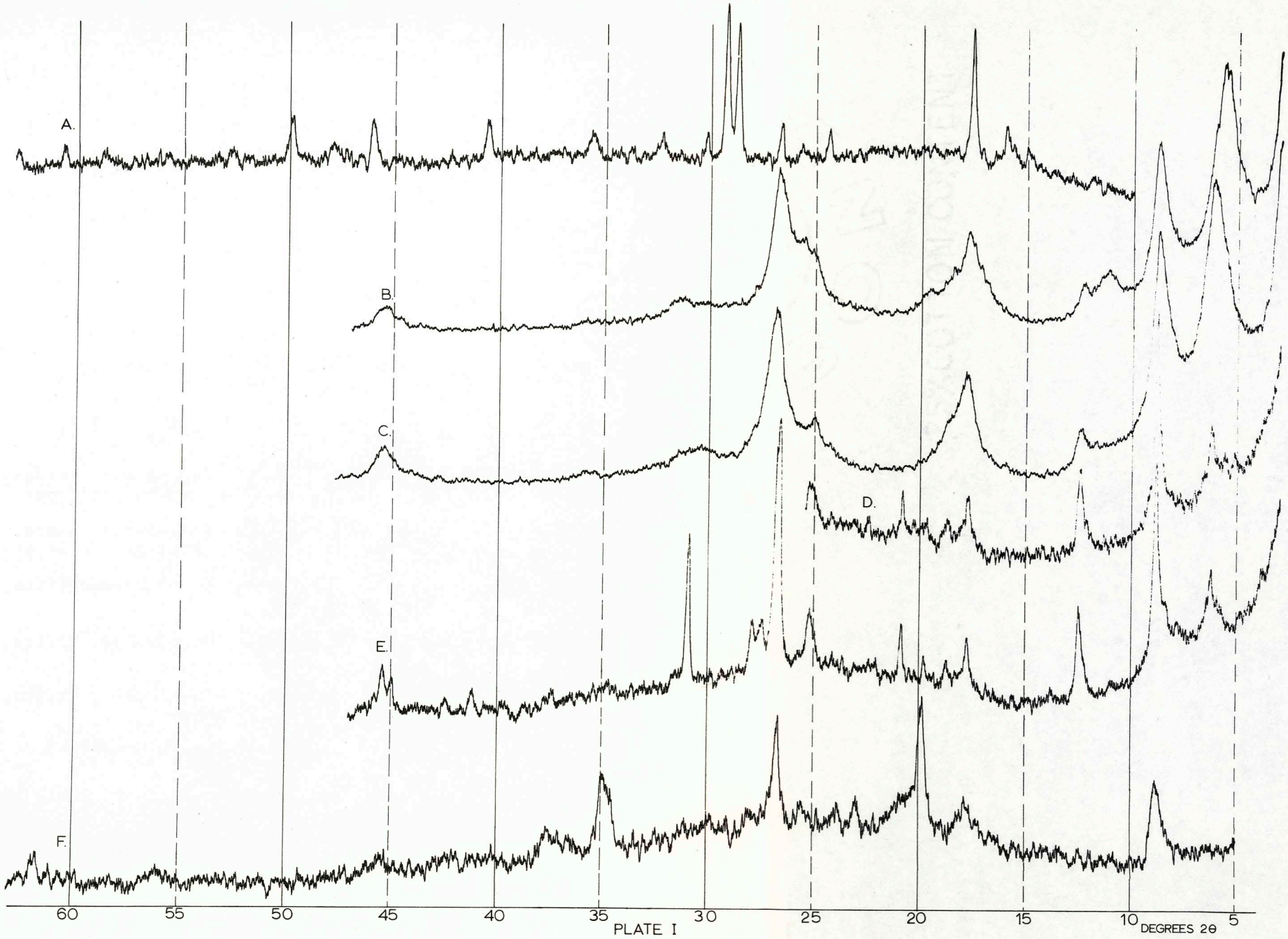

PLATE I

Plate II

SELECTED X-RAY DIFFRACTION PATTERNS

A. A-7-a — < 3.7 microns, K^+ treated, sedimented, solvated; Illite, Chlorite

B. A-7-a — < 3.7 microns, K^+ treated, sedimented, humidified; Illite, Chlorite

C. A-7-a — < 3.7 microns, natural, sedimented, solvated; Illite, Chlorite, Quartz, Feldspar

D. A-7-a — < 3.7 microns, natural, sedimented, humidified; Illite, Chlorite, Quartz, Feldspar

E. A-13-p-1 — gross clay, sedimented, humidified; Illite, Chlorite, Dolomite

F. A-9-b-1 — gross clay, sedimented, humidified; Illite, Chlorite, Dolomite

G. A-2-a — gross clay, sedimented, humidified; Illite, Chlorite, Quartz, Dolomite

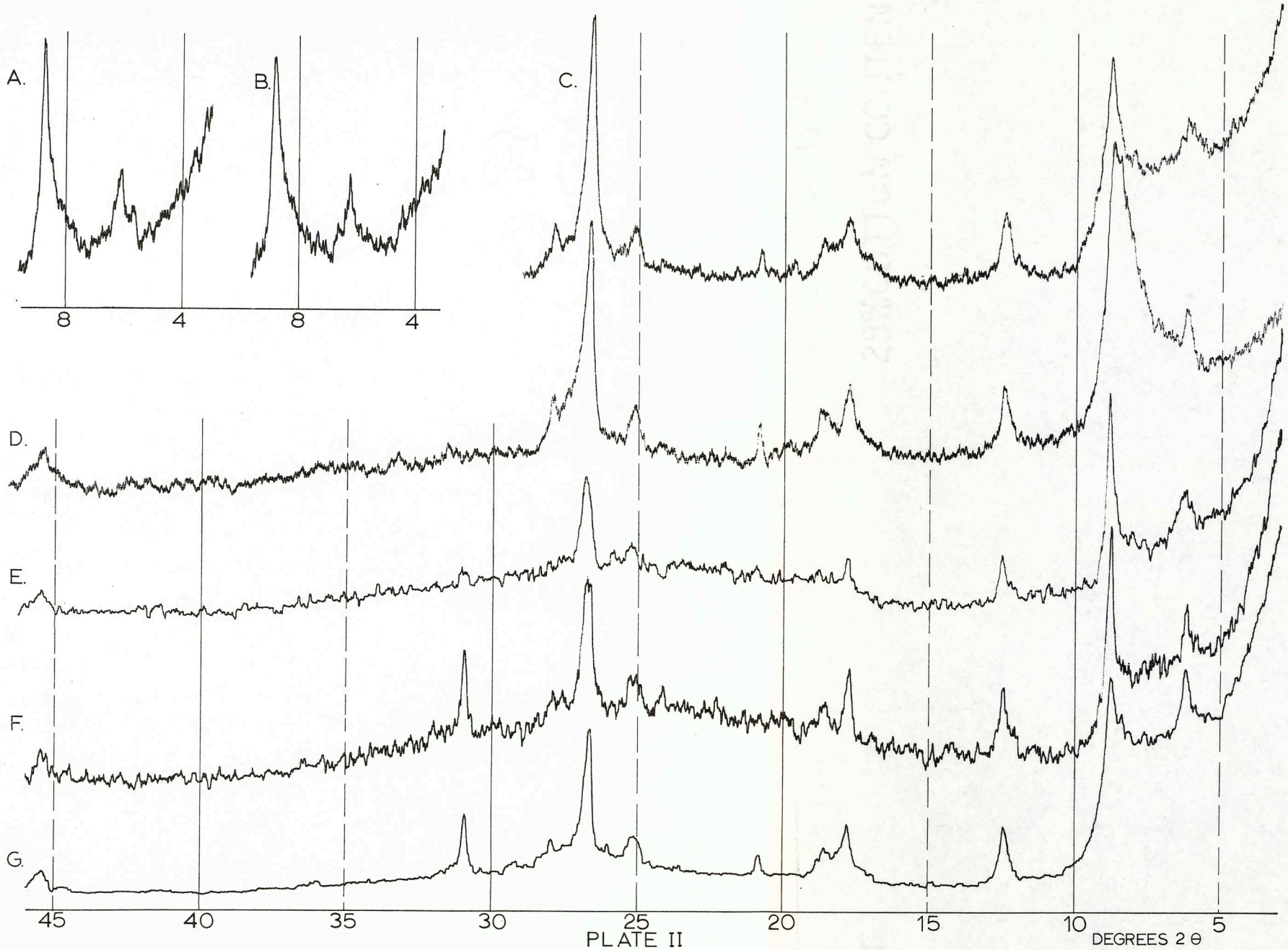

PLATE II

Plate III

DIFFERENTIAL THERMAL ANALYSIS PATTERNS

A.	A-13-c	<3.7 microns; Illite, possible Chlorite
B.	A-7-a	<3.7 microns; Illite
C.	A-13-p-5	¼-½ micron; Illite, altered Illite
D.	C-3-b	<¼ micron; Illite, Chlorite/Vermiculite
E.	C-3-b	¼-½ micron; Illite, Chlorite/Vermiculite
F.	C-3-b	½-1 micron; Illite, possible Chlorite
G.	C-3-b	1-4 microns; Illite, Dolomite
H.	A-13-p-5	Natrojarosite

(A and H run at machine settings of 1.5 X 150, others at 1 X 150)

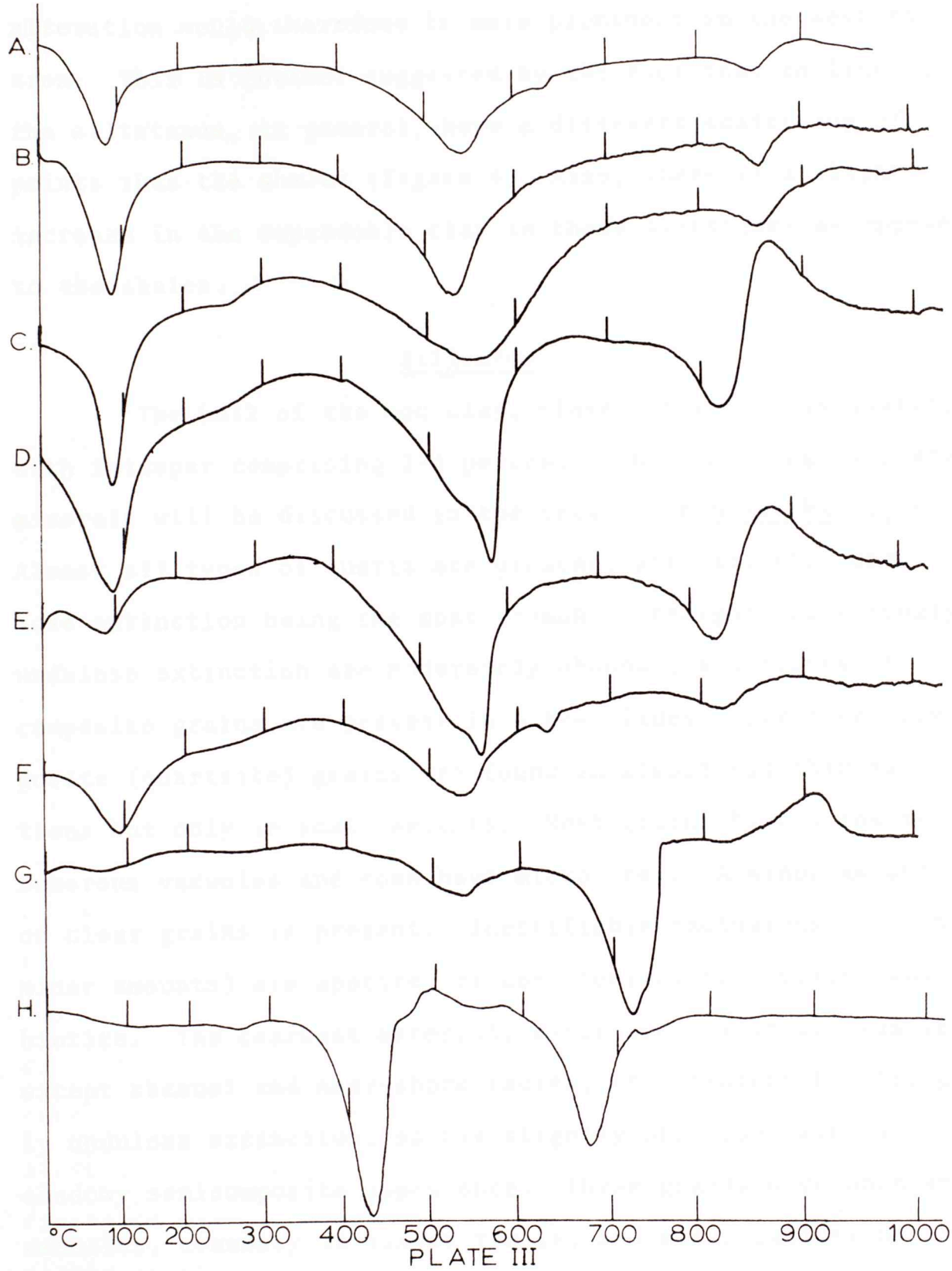

PLATE III

which would slightly increase the permeability. Fluid-derived alteration would therefore be more prominent in the western area. This is further suggested by the fact that in line C, the siltstones, in general, have a different scattering of points than the shales (figure 4). Also, there is a slight increase in the expandable clay in these siltstones as opposed to the shales.

Silicates

The bulk of the non-clay, clastic material is quartz, with feldspar comprising 1-4 percent. The remaining silicate minerals will be discussed in the section on Heavy Minerals. Almost all types of quartz are present, with slightly undulose extinction being the most common. Straight and strongly undulose extinction are moderately abundant and traces of composite grains are present in a few slides. Stretched composite (quartzite) grains are found in almost all thin-sections but only in small amounts. Most grains have a few to numerous vacuoles and some have microlites. A minor amount of clear grains is present. Identifiable inclusions (all in minor amounts) are apatite, zircon, tourmaline, rutile, and biotite. The coarsest material, minor amounts in all samples except channel and near-shore facies, has straight to strongly undulose extinction, mainly slightly undulose, with a shadowy semicomposite appearance. These grains have abundant vacuoles, commonly in linear trails, and minor inclusions of

zircon and apatite. Their size, location, associated feldspar, and shadowy extinction indicate they were derived from the Wichita Mountains.

Quartz-overgrowths are present in approximately one-third of the thin-sections but are normally faint and in minor amounts. The overgrowths are clear and show no zonation or euhedral terminations. Commonly minute carbonate grains are enclosed along the overgrowth-grain boundary.

In the bulk of the formation, orthoclase and plagioclase are present in approximately equal amounts together with a minor amount of microcline. The grains are mostly fresh to slightly altered with minor amounts of all stages of alteration, including highly vacuolized. The larger grains are normally more altered than the smaller and the feldspar alteration sequence is normally orthoclase-most, plagioclase, and microcline-least. Albite twinning and traces of Carlsbad twinning are found in the plagioclase and quadrille twinning in microcline. Only one grain of plagioclase was identified and that as oligoclase. The extinction from the albite twinning was almost always asymmetrical but indicated that most of the grains were in the range albite-andesine. The feldspar in one channel sample, and in scattered sand-sized grains in a few other thin-sections, consists of perthite with minor amounts of anti-perthite and traces of plagioclase and myrmekite. Microcline is identifiable in some of the perthite. Most of these grains are

highly altered or vacuolized, including the microcline, whereas the silt-sized microcline is normally quite fresh to slightly altered. Perthite, anti-perthite, myrmekite, and microcline are common in the granites of the Wichita Mountains.

Feldspar-overgrowths were positively identified in only one thin-section. They are clear, faint, and in trace amounts; no zonation or terminations are shown.

Both quartz and feldspar show minor replacement by carbonate, mainly dolomite. Quartz and feldspar are embayed along the grain margins and the feldspar is also replaced along cleavage planes. Traces of sericitization of quartz are found in a few slides.

Carbonates

The bulk of the carbonate in the Hennessey is dolomite. Calcite is the sole carbonate in only one sample but is dominant in several others. The calcite is poikilitic in two thin-sections and obviously recrystallized in two others. Dolomite occurs both as anhedral grains from 5 to 60 microns and as 10 to 60 micron rhombs. Twinning is not present. Traces of either siderite or iron-stained dolomite were found in heavy mineral separation. The quantity was not sufficient for x-ray identification. The carbonates comprise more than 50 percent of the rock in three samples, two solely dolomite and one mainly calcite with minor dolomite.

Carbonate comprises 20-35 percent of the siltstones and zero to approximately 50 percent of the shales.

Sulfates

Gypsum occurs throughout the formation, particularly in core samples, in all three crystal habits. Selenite crystals up to one inch in size cover the ground at many outcrops. These are probably formed by weathering and leaching. Thin veins and stringers of both selenite and satin spar are found mainly in the cores and, in places, at the surface. Nodular, white and pink, granular concretions are likewise found both at the surface and in the cores. Gypsum was identified as a cementing material in only 1 of 22 thin-sections where it occurs as satin spar and small fibers disseminated through the matrix.

Barite also is found in three different habits, but only in trace amounts. Clear cleavage plates and granular cement were found in several heavy mineral separations. These two types are not observed in thin-section. Round, pink nodules are prominent in one sample and questionably identified in three or four other samples. These nodules are oolitic in appearance, with a radial, fibrous structure, normally around a silt core. Some are broken or crushed. In size, these oolitic nodules range from 1.5-4.0 Ø.

Two samples of limonitic zones in the upper Hennessey contain a member of the jarosite family. It forms

yellow, granular crusts in association with limonite and gypsum. X-ray data are similar to jarosite, $KFe_3(SO_4)_2(OH)_6$; natrojarosite, $NaFe_3(SO_4)_2(OH)_6$; and carphosiderite, (H_2O) $Fe_3(SO_4)_2(OH)_5$. Unit cell parameters computed from (006) and (220) spacings of 2.771 Å and 1.827 Å give 16.626 Å for "c_o" and 7.308 Å for "a_o". Emission spectrographic analysis gives a sodium-potassium ratio of 2.14 to 1. In addition, DTA data indicate a minor water loss in the range of 230°-280°C (plate III).

A recent paper by Brophy and Sheridan (1965) includes a summary of the present knowledge of the jarosites. The mineral carphosiderite has been discredited and shown to be a hydronium-bearing natrojarosite. The jarosite family of the alunite group is composed of basic alkali iron sulfates. There is a solid substitution series of K^+-Na^+-H_3O^+, the end members of which define the minerals of the family. Using the (006) and (220) spacings Brophy and Sheridan determined the "c_o" and "a_o" unit cell dimensions on a large number of natural and synthetic jarosites and arrived at the following data:

"a_o" - H_3O^+-7.355 Å, Na^+-7.312 Å, K^+-7.288 Å

"c_o" - K^+-17.192 Å, H_3O^+-16.980 Å, Na^+-16.620 Å

Also, they determined that, on heating, the amount of water lost between 240°-280°C was the amount of H_3O^+ ion involved in the substitution.

From the spectrographic analysis data the mineral is

natrojarosite. Close agreement of the "a_o" and "c_o" parameters with those published by Brophy and Sheridan confirm this. DTA data indicates minor hydronium substitution giving an approximate formula of $[K_{.29}Na_{.61}(H_3O)_{.10}]\,Fe_3(SO_4)_2(OH)_6$. Synthesis data show that it is a low-temperature, low-pressure mineral. Formation probably resulted from the oxidation of pyrite and chlorite in the presence of gypsum.

Heavy Minerals

General Statement

Nine siltstones and one argillaceous limestone were examined for heavy minerals. These made up less than one percent of the sample in all cases. Although the bulk of the heavy mineral suite is composed of ultra-stable minerals, there are numerous metastable and some unstable minerals present (table 3).

Titanium Dioxide Minerals

Rutile, brookite, and anatase are all present in the Hennessey. Rutile is present in all forms from anhedral to euhedral, including geniculate twins. Most is yellow, but traces of red and red-brown, rounded grains are present. Anatase is identical to the yellow varieties of rutile and is identified by its uniaxial negative character. Brookite is yellow, rectangular; has anomalous yellow and blue, metallic birefringence; and shows crossed dispersion.

	C-9-c	C-9-f	C-9-j	C-9-m	C-10-a*	C-3-b	C-1-a-2*	A-15-b	A-4-a	A-13-e-1
TiO_2	45.3	47.5	42.4	40.3	41.1	50.0	42.0	48.4	abun	abun
Tourmaline	30.5	35.6	34.5	13.3	17.4	15.1	22.6	17.9	min	mod
Zircon	3.3	3.2	2.0	7.7	9.9	1.0	8.2	12.0	min	mod
Garnet	16.7	8.1	4.6	6.3	18.4	2.0	9.2	13.3	tr	mod
Opaques	0.3	0.9	3.0	27.0	8.8	0.3	8.6	1.2	abun	abun
Chlorite	1.6	0.3	3.6	2.3	tr	27.3	3.0	0.3	tr	tr
Staurolite		tr	tr		0.7	tr	tr	0.3		tr
Pyrite		tr		0.3	0.3	tr	0.7	1.9	tr	
Sphene	tr	0.3				0.3		tr		tr
Biotite			1.3	tr		1.3	0.3		tr	
Amphibole/ Pyroxene	1.3			0.3			0.3	0.3		
Muscovite		tr		tr	0.3	0.7	2.3			
Barite	0.7	2.6	8.3	1.0	1.3	0.3	0.7	3.0	tr	min
Carbonate		1.3	tr	0.7	0.7		1.6			

TiO_2 includes leucoxene, rutile, anatase, and brookite.

Opaques include hematite, ilmenite, and magnetite.

Carbonate is iron-stained, may be siderite.

*non-HCl-treated, percentages adjusted for apatite content.

tr-trace, present in slide but not in grain count.
abun-abundant, mod-moderate, min-minor.

HEAVY MINERAL PERCENTAGES

Table 3

Brookite is found in traces, x-ray data show rutile and anatase approximately equal. Most of the above grains seem to be clastic.

Although the counts of rutile (including anatase and brookite) and leucoxene are widely divergent, the total percentage of these minerals is more constant (figure 5). High magnification shows that most of the leucoxene-like grains contain granules or short fibers of crystalline material. This material ranges from microlites on the edge of a leucoxene grain through granules and short fibers randomly scattered throughout the grain to a net of needle-like crystals in sets intersecting at angles of approximately 60°. X-ray data indicate large amounts of rutile and anatase and essentially no amorphous material. As indicated in figure 5, high counts of rutile commonly coincide with low percentages of leucoxene and vice versa. This variation is due to the gradations of rutile content in many of the leucoxene grains and the difficulty in placing some grains in one category or the other. Grains of leucoxene containing microlites of rutile and anatase are generally thought to indicate recrystallization of rutile and anatase from leucoxene (Tyler and Marsden, 1938).

Tourmaline

The tourmaline group is the most numerous of those heavy minerals found in the Hennessey that are useful for

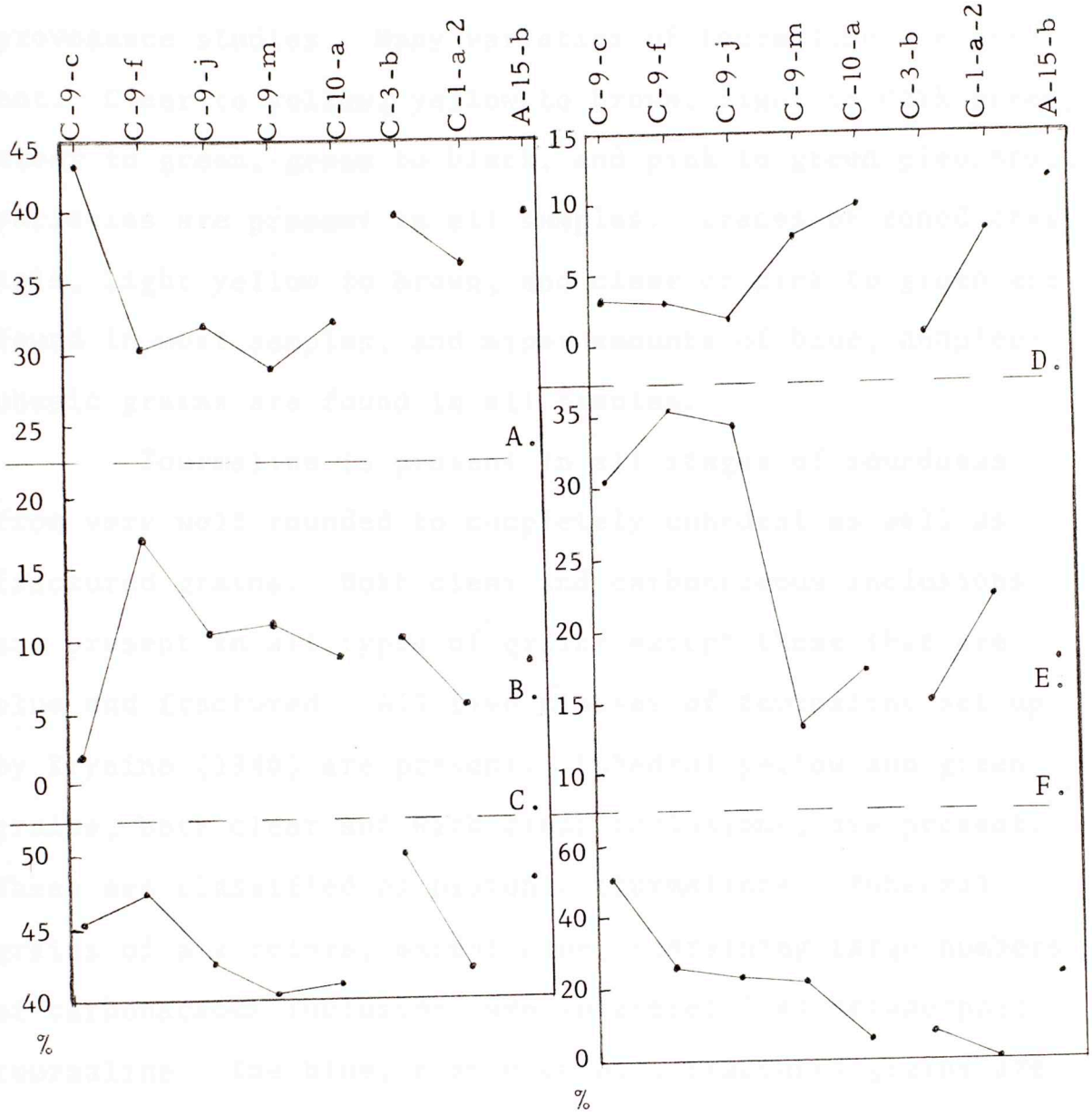

A. Leucoxene
B. Rutile
C. Total TiO_2 Minerals
D. Zircon
E. Tourmaline
F. Percentage Euhedral Tourmaline Grains (of total Tourmaline)

C-3-b equivalent to C-9-j
C-1-a-2 equivalent to C-10-a

SELECTED HEAVY MINERAL TRENDS

Figure 5

provenance studies. Many varieties of tourmaline are present. Clear to yellow, yellow to brown, light to dark green, clear to green, green to black, and pink to green pleochroic varieties are present in all samples. Traces of zoned crystals, light yellow to brown, and clear or pink to green are found in most samples, and minor amounts of blue, nonpleochroic grains are found in all samples.

Tourmaline is present in all stages of roundness from very well rounded to completely euhedral as well as fractured grains. Both clear and carbonaceous inclusions are present in all types of grains except those that are blue and fractured. All five classes of tourmaline set up by Krynine (1946) are present. Euhedral yellow and green grains, both clear and with clear inclusions, are present. These are classified as plutonic tourmalines. Euhedral grains of all colors, except blue, containing large numbers of carbonaceous inclusions are interpreted as metamorphic tourmaline. The blue, nonpleochroic, fractured grains are probably of pegmatitic origin. Traces of possible rounded tourmaline-overgrowths are found in a couple of samples. All varieties of tourmaline, except blue, are found as rounded, subhedral to completely anhedral and broken grains and are interpreted as reworked sedimentary grains. These are mainly of original plutonic derivation with moderate amounts of metamorphic tourmaline. The euhedral grains, on the other hand, are roughly one-half plutonic and one-half

metamorphic.

The only trend that can be established is in the siltstones in the western portion of the area. There, the percentage of euhedral grains (both plutonic and metamorphic) decreases from the bottom to the top of the sequence (figure 5). The ratio of plutonic to metamorphic grains remains constant.

Zircon

Although zircon is an ultra-stable mineral, it is present in the Hennessey only in minor amounts (table 3). The bulk of the zircon grains are colorless, but traces of pink grains are present. Both clear and zoned grains are present with the clear ones predominant but decreasing toward the top. A few grains are euhedral, both clear and zoned. The bulk of the grains are subhedral to anhedral and rounded. A larger percentage of the clear grains are euhedral than the zoned grains. The light pink grains are almost spherical, never subhedral or euhedral. Zircons seem to increase toward the top of the formation (figure 5).

Garnet

Most of the garnets are colorless, angular, and moderately to highly etched. A few are subhedral to anhedral, rounded, and may or may not be etched. Also, traces of pink, round grains and clear, euhedral grains are found.

Opaque Minerals

Opaque minerals are normally of little value in provenance studies. For this reason and because of the difficulty in distinguishing between ilmenite and magnetite, they have been counted together along with hematite. Much of the hematite is authigenic, pseudomorphic after pyrite, as shown by its cubic shape.

Important Accessory Minerals

Staurolite. Although staurolite is found only in traces in seven of the 10 analyses, it is nonetheless a valuable provenance indicator. The grains are faintly pleochroic, clear to light tan with a low birefringence, and optically biaxial with a large 2V. The shape of the grains is characteristic of detrital staurolite, elongate, hackly edges formed by the combination of cleavage and solution. Their presence indicates derivation from regionally metamorphosed sedimentary rocks.

Chlorite. Normally the micas are not included in heavy mineral counts. However, in quantity, chlorite indicates a metamorphic source. It is found in measurable or trace amounts in all 10 analyses. The grains are thin cleavage flakes that are oval to round. There are few broken, angular fragments. Clear, light and dark green grains are found, whose 2V is very low to uniaxial and whose optical character is negative where determinable. The

interference figure is indistinct in most grains. Due to the hydraulic behavior of micas and susceptability of chlorite to destruction by HCl, no conclusions were drawn from the widely differing percentages found in the 10 samples analyzed.

Apatite. Abundant percentages of apatite were found in the non-acidized samples (14.4 in C-10-a and 9.8 in C-1-a-2). Subsequent reexamination of non-acidized portions of samples C-3-b and C-9-f also showed abundant apatite. As this mineral is so highly susceptable to destruction by HCl, the percentages of it are not reported and samples C-10-a and C-1-a-2 were recomputed on an apatite-free basis to agree with the other analyses.

The apatite found in the Hennessey is in clear, oval to spherical grains with no visible inclusions.

Trace Accessory Minerals

Barite is present in the samples and was discussed in the section on Sulfates. Pyrite is found in trace amounts in most of the samples. In most cases, noticeable pyrite occurred in those samples with a moderate or high opaque mineral percentage. Muscovite and biotite are present in trace amounts in roughly one-half of the analyses. As mentioned under Chlorite, the hydraulic behavior of the micas is too uncertain to attach much significance to their percentages. Sphene, likewise, is found as clastic grains in

one-half of the analyses. The occurrence of sphene is limited to those samples with the highest total TiO_2 percentages.

Amphibole and/or pyroxene was identified in four samples and possibly in two others. Hornblende is present in one sample and a green pyroxene in another. The remaining grains are too few for identification as to group or individual mineral.

Evaluation of the Heavy Mineral Suite

Approximately one-half of the heavy minerals are authigenic - leucoxene, recrystallized rutile and anatase, pyrite, and hematite. The majority of the remaining grains are the ultra-stable group, tourmaline and zircon, that show moderate to extreme rounding. Euhedral metamorphic and plutonic tourmaline and zircon (acid igneous source) are present in minor amounts, decreasing toward the top of the formation. Moderate to abundant garnet and traces of staurolite also indicate a metamorphic source as does abundant detrital chlorite. Traces of pegmatitic tourmaline are found.

The source area as indicated by the heavy minerals has a complex lithology. Sedimentary sources are approximately equal to primary metamorphic/plutonic areas in the upper one-third of the Hennessey but increase in importance higher in the section, as shown by tourmaline ratios

(figure 5, F). The sedimentary source itself is compound, being derived from both igneous and metamorphic rocks. The metamorphic areas contain at least some metamorphosed sediments. Minor areas of pegmatite are also indicated.

Plate IV

SELECTED PHOTOMICROGRAPHS

A. A-15-b.
Euhedral metamorphic tourmaline grain.
plane polarized light
(X250)

B. A-13-e-1.
Staurolite grain.
plane polarized light
(X250)

C. C-9-f.
Two etched garnet; one euhedral plutonic tourmaline; and subhedral and anhedral tourmaline grains.
plane polarized light
(X100)

D. A-13-e-1.
Euhedral garnet; two subhedral, unetched garnet; and one zoned zircon grain.
plane polarized light
(X100)

E. A-13-e-1.
Clastic barite nodule.
plane polarized light
(X100)

F. C-9-c.
Altered perthite grain, medium sand.
plane polarized light
(X25)

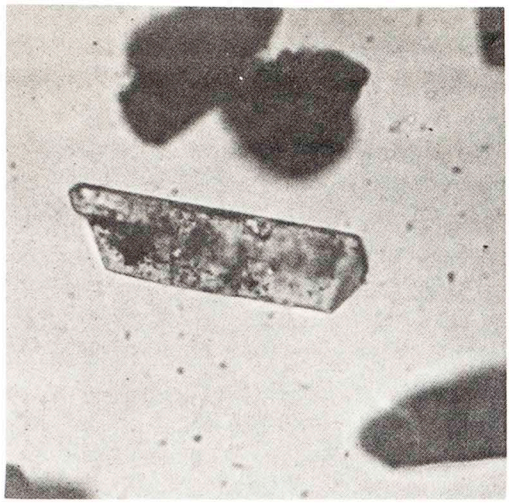

A.

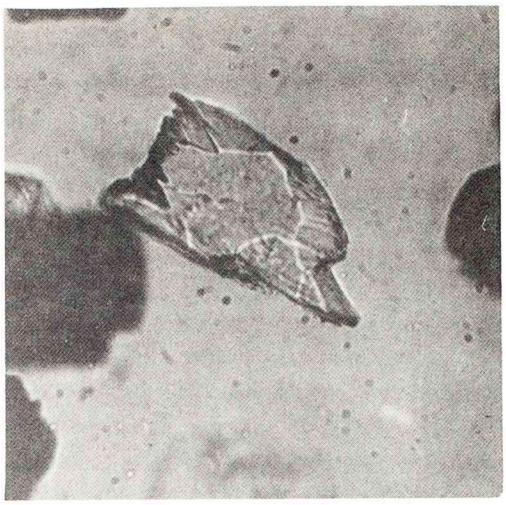

B.

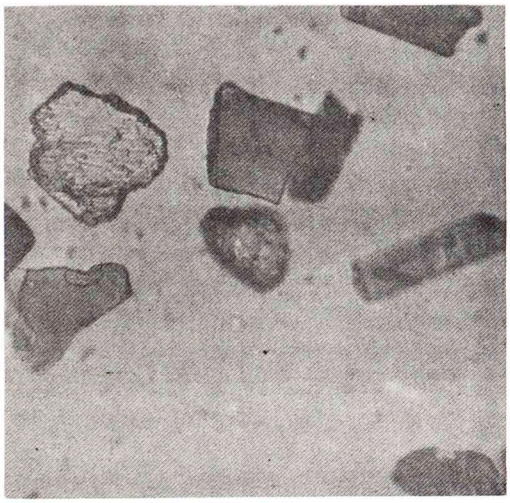

C.

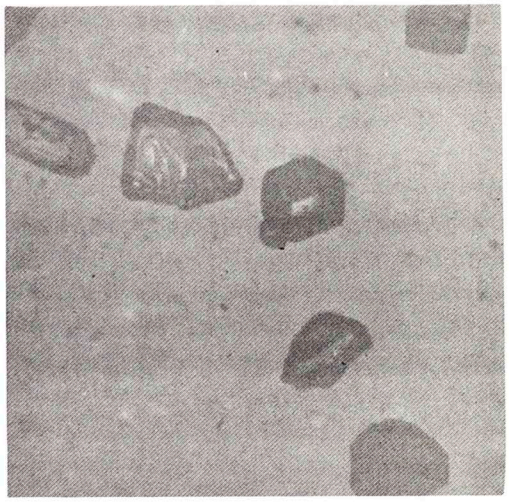

D.



E.

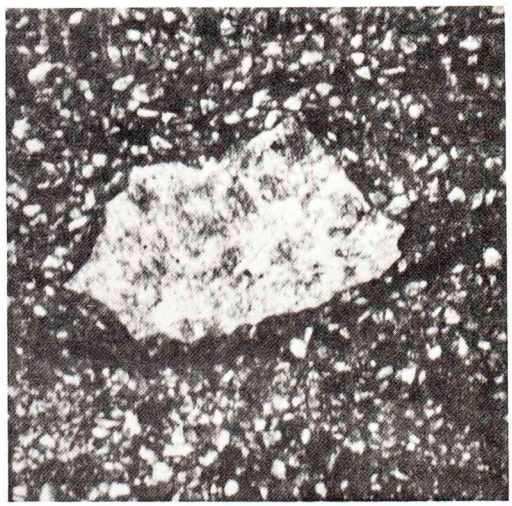

F.

PLATE IV

Plate V

SELECTED PHOTOMICROGRAPHS

A. A-13-e-1.
Metaquartzite (upper center) and quartz-mica schist (lower center) grains.
crossed nicols
(X250)

B. C.H. AL-1-6.
Well-oriented clay intraclast set in siltstone, sectioned parallel to bedding.
plane polarized light
(X25)

C. B-4-a-2.
Clay/silt lamination, cross-bedding.
plane polarized light
(X10)

D. C-9-j.
Placer concentration of opaque minerals, bedding disruption by burrowing.
plane polarized light
(X25)

E. C-6-d-3.
Quartz, highly altered perthite set in sparry dolomite and clay and microgranular dolomite cement.
crossed nicols
(X10)

F. C.H. AL-2-5.
Micritic intraclasts set in a micrite and silt matrix, differential iron oxide-staining between intraclasts and matrix, recrystallized.
plane polarized light
(X25)



A.

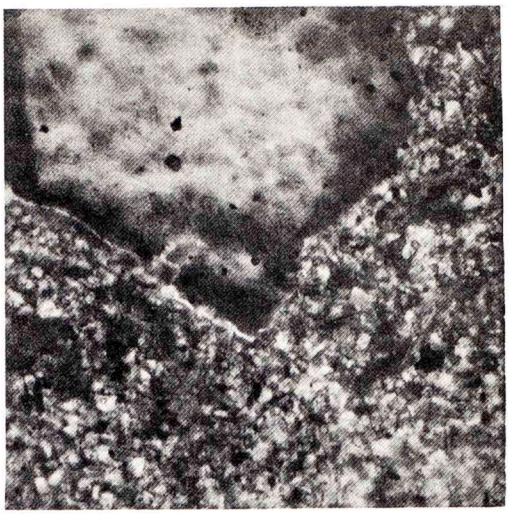

B.

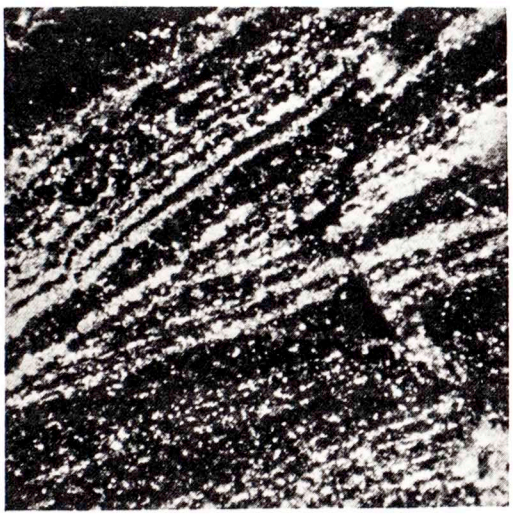

C.

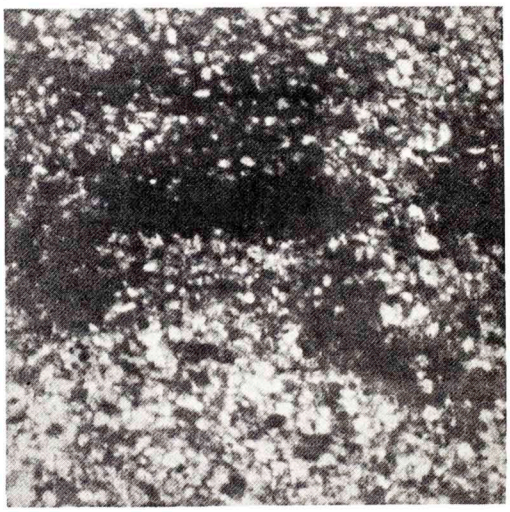

D.

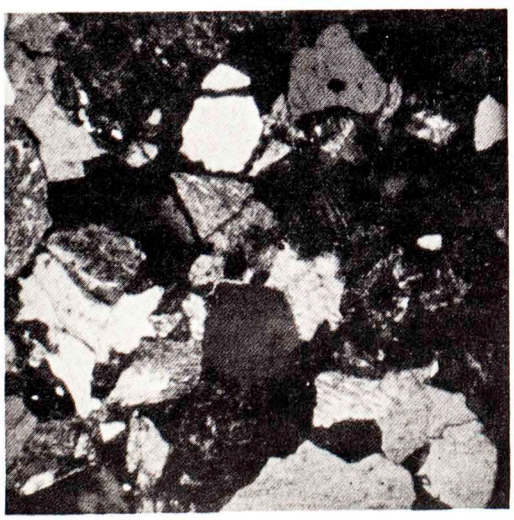

E.



F.

PLATE V

PETROGRAPHY

Siltstones

Except for a few channel and near-shore beds, the coarsest rocks in the Hennessey are siltstones. They are immature, coarse to fine silt, commonly laminated to very thin-bedded. Most are orthoquartzites but some are subgraywackes and subarkoses. The grains are angular to round; subequally angular and subangular, moderately subround with traces of round grains. Quartz is the dominant clastic component, feldspar 1-4 percent, and rock fragments 1-3 percent. Metamorphic rock fragments are quartzite, quartz-chlorite schist, and quartz-muscovite schist. These are normally smaller and more rounded than the quartz grains. Sedimentary intraclasts are mainly clay-carbonate with some clay grains and carbonate grains. These are commonly fine sand to coarse silt-sized and range from round to angular, with many flattened grains. The carbonate intraclasts show recrystallization.

Bedding is shown by most slides but in varying degrees. Some are extensively disrupted, probably by burrowing. Mica and clay orientation is the most prominent

lamination, but alignment of intraclasts and segregation of silt and clay in different laminae are also prominent. Two slides (A-13-e-1 and A-15-b) have calcite cement with poikilitic texture and show no bedding.

Feldspar grains are about the same size and roundness as the quartz. Many cleavage surfaces are visible. No particular difference in the alteration of the feldspars was noticed between the two slides with poikilitic cement and those without.

The alteration by type of feldspar is somewhat anomalous. Plagioclase is normally less altered than orthoclase but more-so than silt-sized microcline. Coarser grains of all types are more altered than the finer and the sand-sized grains of microcline and perthite are the most altered.

The most common cement is microgranular dolomite, but euhedral and subhedral dolomite is predominant in some slides. The euhedral grains replace microgranular cement and occur as isolated grains in the clay matrix. In samples containing both calcite and dolomite, as shown by x-ray data, only a few rhombs are found. Dolomite apparently formed first as an anhedral alteration of calcite and then later recrystallized.

Both quartz and feldspar-overgrowths are found in the Hennessey, the latter only definitely identified in one slide. The quartz-overgrowths were formed after the carbonate cement as many contain grains of carbonate along the

grain-overgrowth boundary. Overgrowths occur only as a cementing agent between two or more closely packed grains. They are never found on free grain edges.

Numerous grains in most of the thin-sections show a thin clay coating around the grain. The coating is patchy, some close-packed grains being separated by clay whereas others are not. The relationship between overgrowths and coatings is not clear but, in a few instances, the overgrowths seem to contain the clay coating.

Some barite nodules in A-13-e-1 seem to be concretions. However, many are broken fragments and crushed grains that have a clastic appearance. In addition, they are iron-stained whereas the host rock is not. They probably are authigenic concretions that were reworked and deposited as intraclasts in the area in which they are now present.

The one sandstone sectioned is a channel sample (C-6-d-3). The feldspars are highly altered and replaced by calcite. Although this suggests post-depositional alteration, much of it was pre-depositional as the large grains of microcline and perthite throughout the Hennessey are highly altered. There are apparently two generations of cement in this thin-section. The grains are separated from each other and from the large plates of dolomite by thin layers of clay and microgranular carbonate.

Mudstones and Shales

Most of the finer-grained thin-sections are mudstones, but this is because only moderately or highly resistant beds were sectioned. Clay comprises from 10 percent in some of the siltstone to as much as 70 or 80 percent in some of the shales. Both the quartz and feldspar grains show no essential difference between the shale and siltstone. Mudstones and shales are both bedded and nonbedded. Finely laminated cross-bedding is also present. Bedding is shown by mica and clay orientation and by segregation of clay and silt into different laminae. Possible burrowing causes some disruptions. Some samples show nothing but intraclasts of clay and clay-carbonate in a clay, carbonate, and silt matrix.

The red coloration in the shale is due to iron oxide-staining. The staining coats all components of the shale. Thin-section studies show merely a removal of the stain in the green reduction spots, normally with a fairly sharp boundary between reduced and nonreduced areas. Clay orientation in the rock proceeds uninterrupted into the reduction spots and quartz and feldspar grains in both areas have clay coatings. Thin-sections which are mainly intraclasts show both clay and carbonate intraclasts are more deeply stained than the enclosing matrix. The same feature is shown in laminated mudstones where intraclasts are scarce. This indicates that in these samples, at least, the staining is

post-depositional and pre-lithification.

Carbonates

Only three carbonates were found, two surface and one core sample. All show moderate to extreme recrystallization. A-4-a is a cross-bedded, highly argillaceous, dolomitic limestone. Recrystallization is so extreme that no structure is left. Bedding is shown only by streaks of gray mud that is possibly carbonaceous. Some rhombs of dolomite are found but most of the dolomite (as indicated by x-ray data) is indistinguishable from the calcite.

Sample C-5-c is found between two igneous outcrops in the Wichita Mountains. It is a thin, laminated, gray-green claystone that has a layer of gray dolomite nodules in the center. These nodules are 3-4 inches thick and a foot or more in diameter. Banding in the claystone seems to wrap around the nodules. The claystone is mainly dolomite but contains abundant clay. The nodules have less than two or three percent clay, are lithographic, and show no structure. In thin-section, the nodule has no relict structure and seems to be recrystallized micrite with the grains ranging from 5 to 15 microns.

Sample 5 from the AL-2 Core is a dolomitized intramicrite with micritic intraclasts. Recrystallization is evident to the point of removing all structure except the indications of the intraclasts. This rock shows the same staining features as the intraclastic mudstones.

PROVENANCE AND ENVIRONMENTAL STUDIES

Grain Size Analysis

Grain size distributions of nine siltstones and the clastic portion of an argillaceous limestone were examined by sieve and pipette methods (Folk, 1961). The resulting cumulative curves, drawn on probability paper, were similar (figures 6-15). The various statistical parameters are shown in table 4. Mean grain size ranges from coarse to fine silt, but the mode (the most frequently-occurring grain size) ranges only from coarse to medium silt. Inclusive graphic standard deviation, which is a measure of sorting, ranges from poorly to very poorly sorted. All 10 samples are strongly fine-skewed. This is interpreted as an excess of fine material, as can be seen from the "tails" on the cumulative curves. The samples range from very to extremely leptokurtic. This indicates the bulk of the material is better sorted than the coarse and fine material.

Various scatter diagrams of the statistical parameters were made. Three of these show linear trends (figure 16). Standard deviation increases as the mean grain size decreases, which indicates the finer grained siltstones are

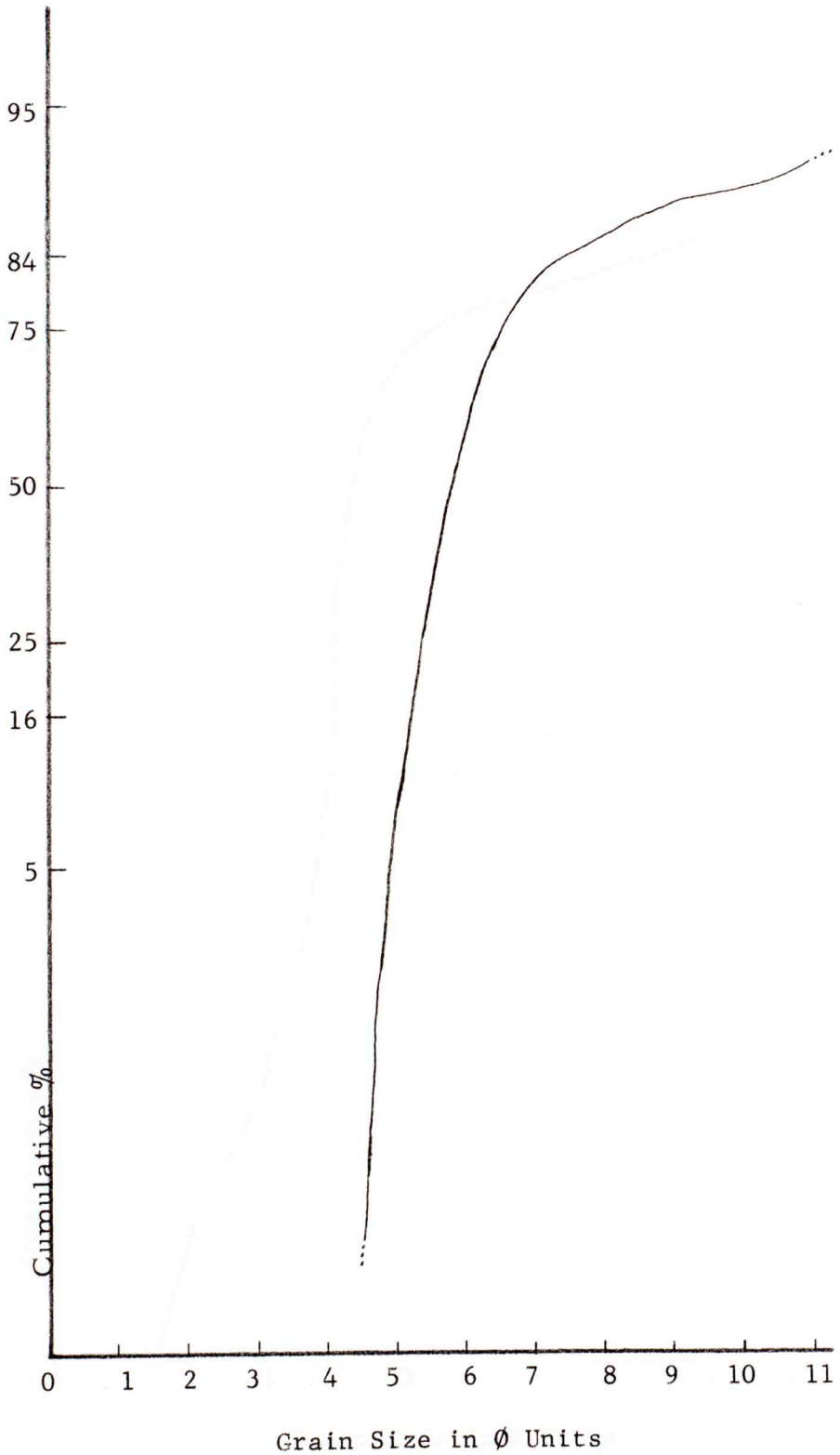

A-4-a

GRAIN-SIZE DISTRIBUTION, CUMULATIVE CURVE

Figure 6

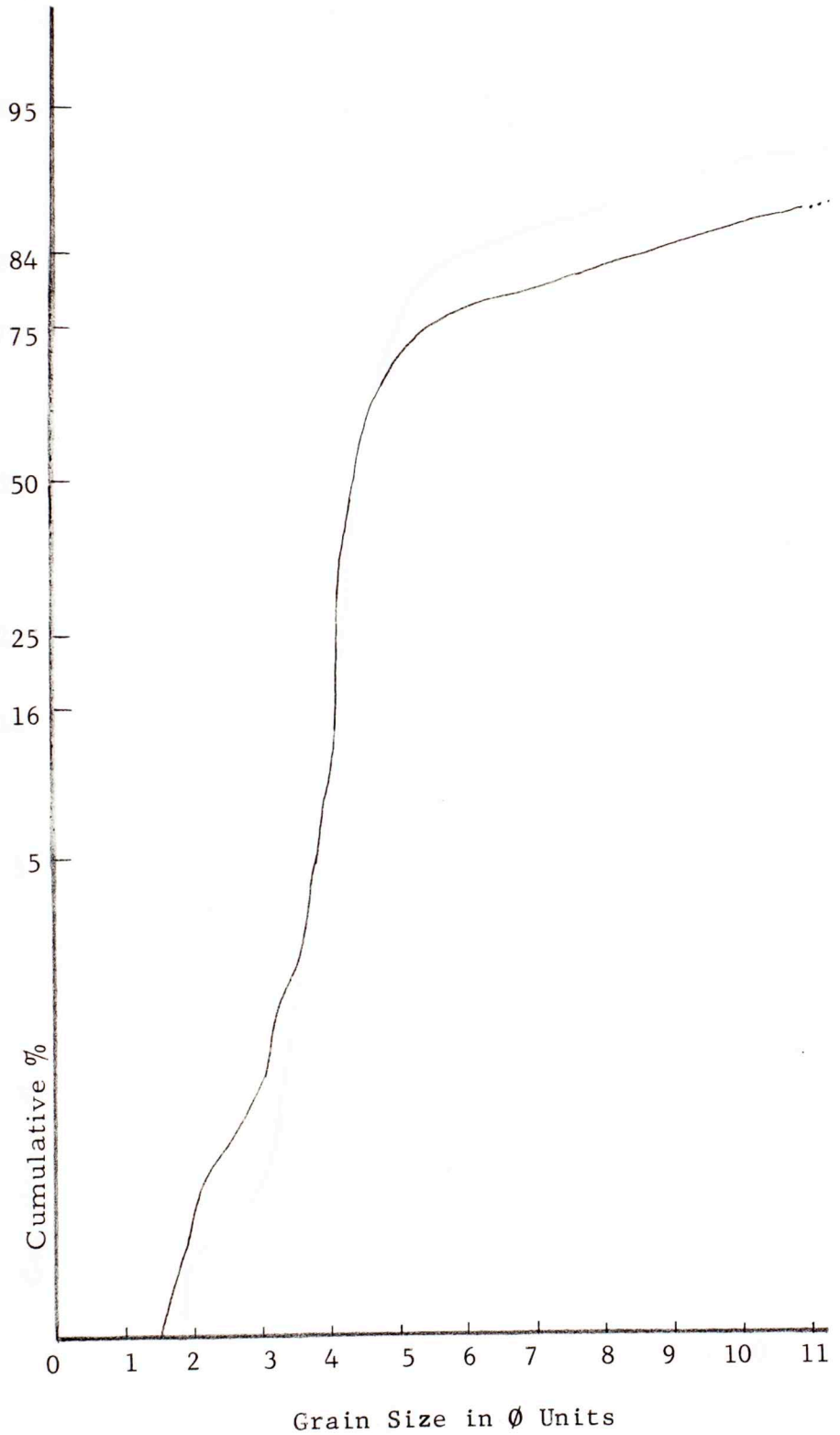

A-13-e-1

GRAIN-SIZE DISTRIBUTION, CUMULATIVE CURVE

Figure 7

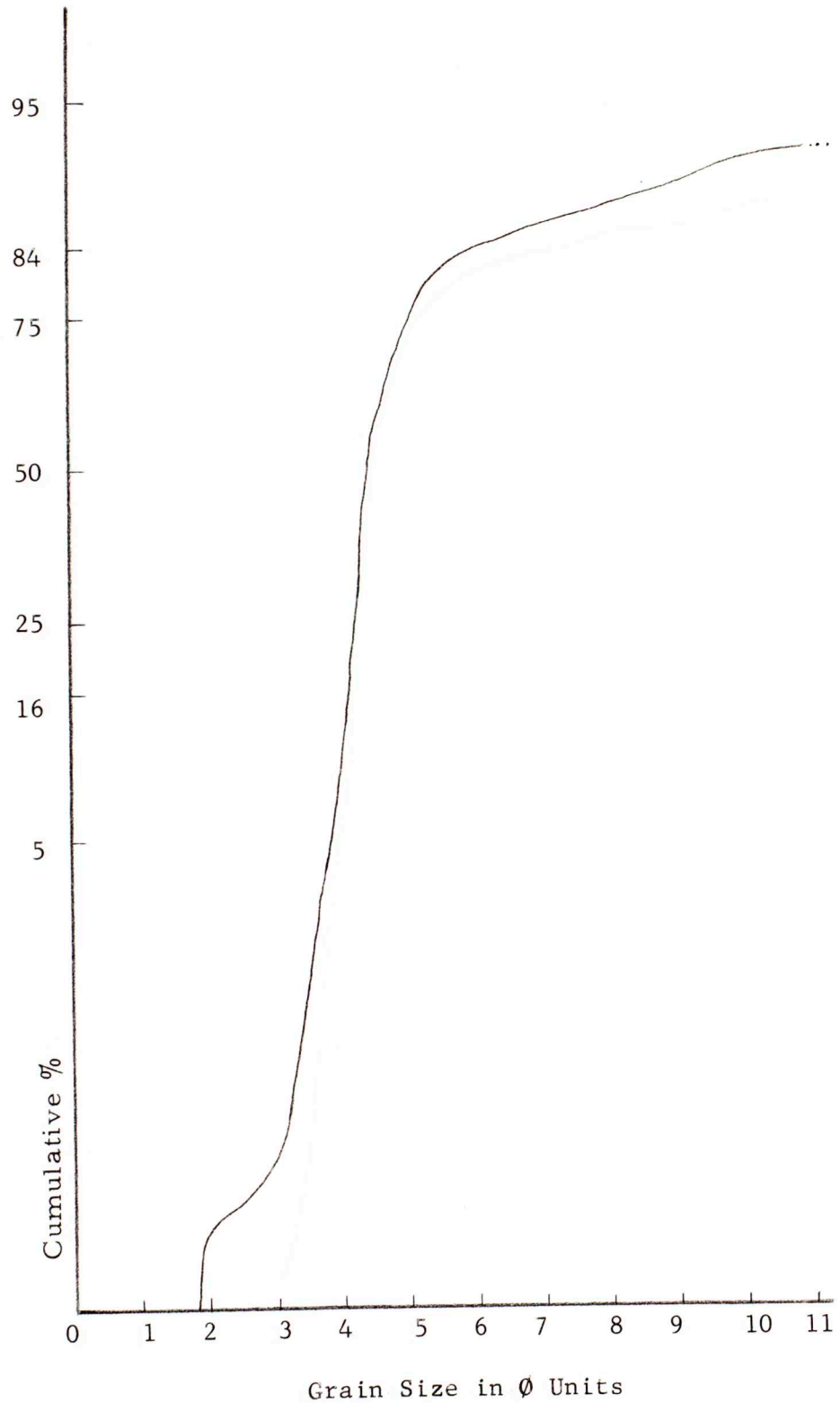

A-15-b

GRAIN-SIZE DISTRIBUTION, CUMULATIVE CURVE

Figure 8

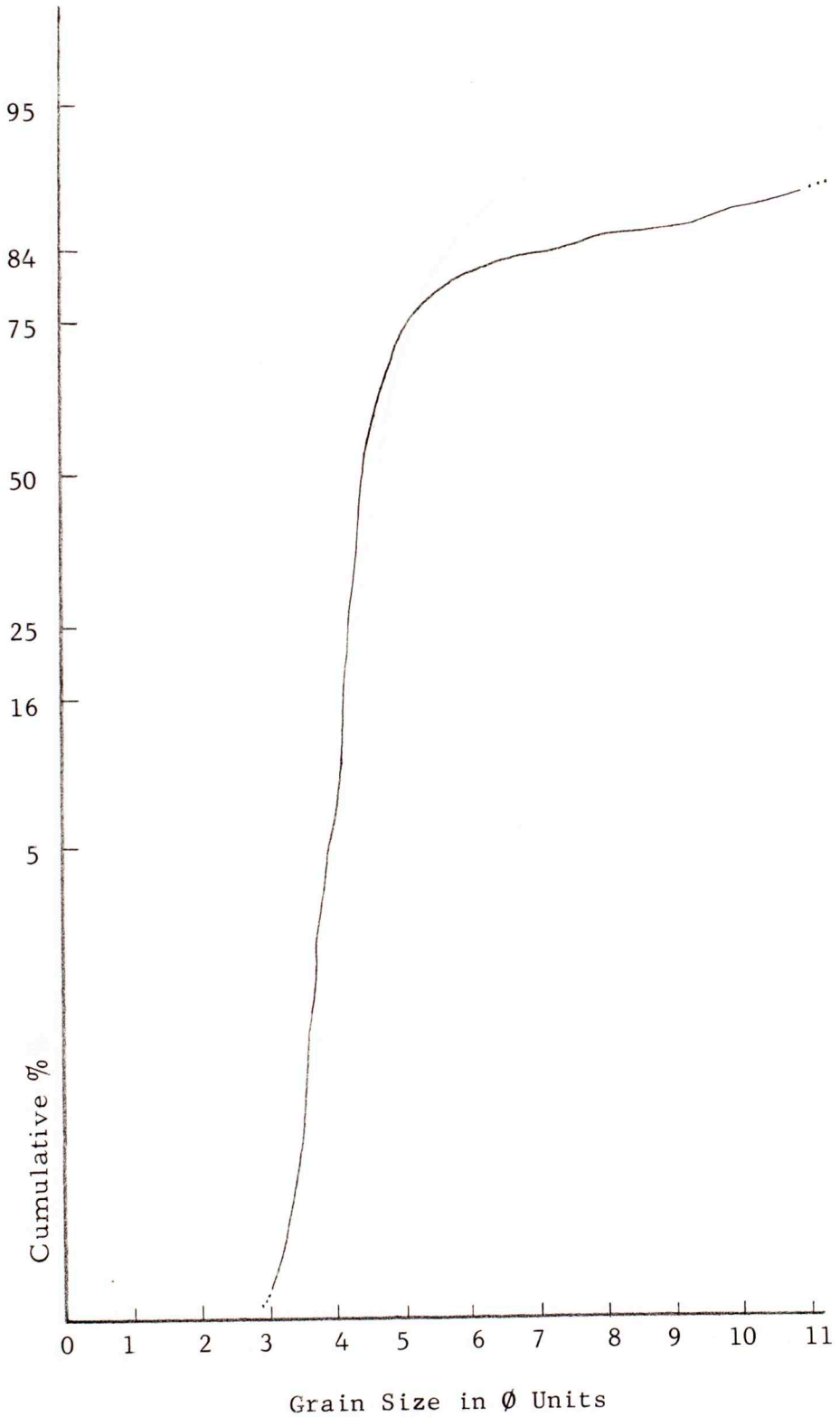

C-1-a-2

GRAIN-SIZE DISTRIBUTION, CUMULATIVE CURVE

Figure 9

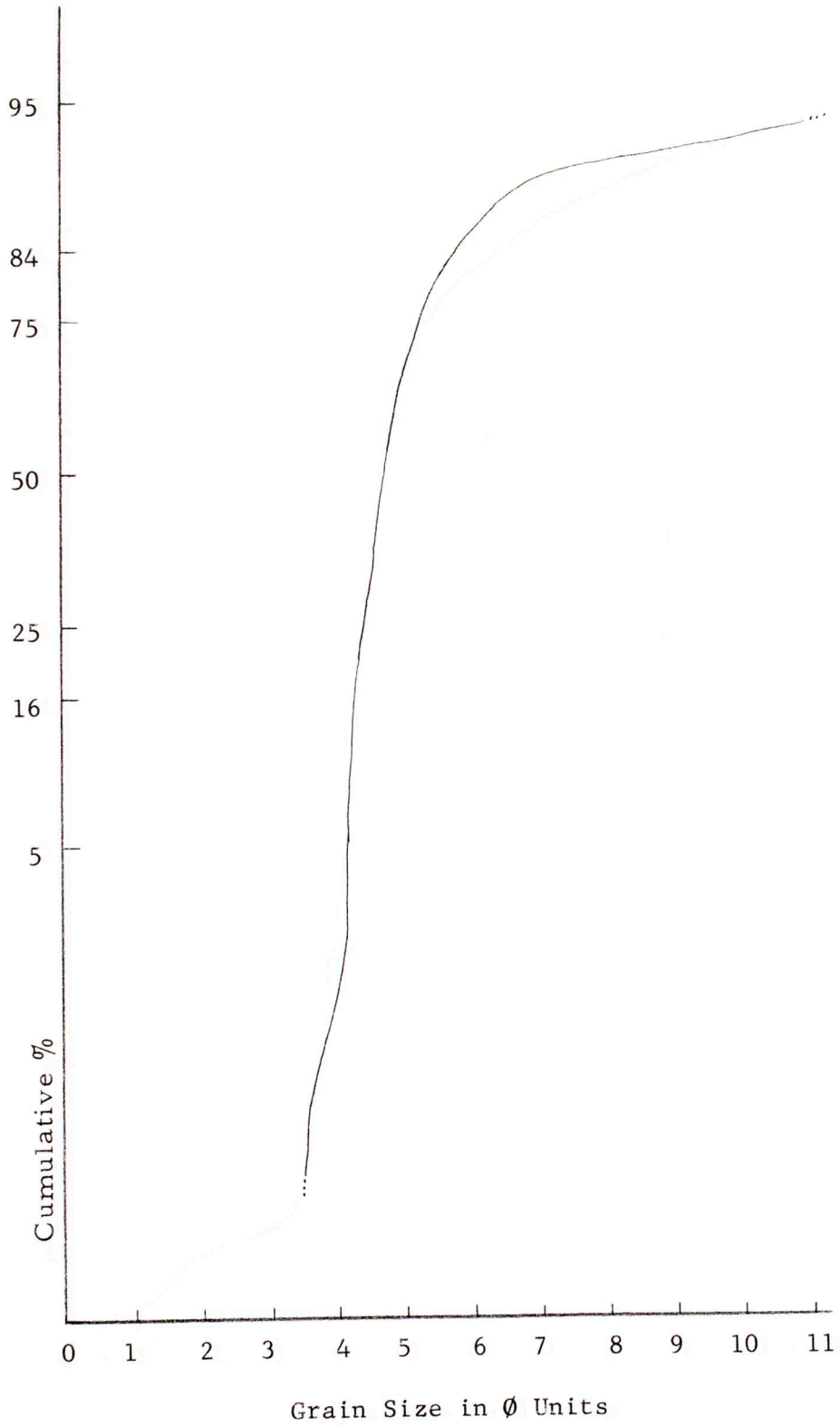

C-3-b

GRAIN-SIZE DISTRIBUTION, CUMULATIVE CURVE

Figure 10

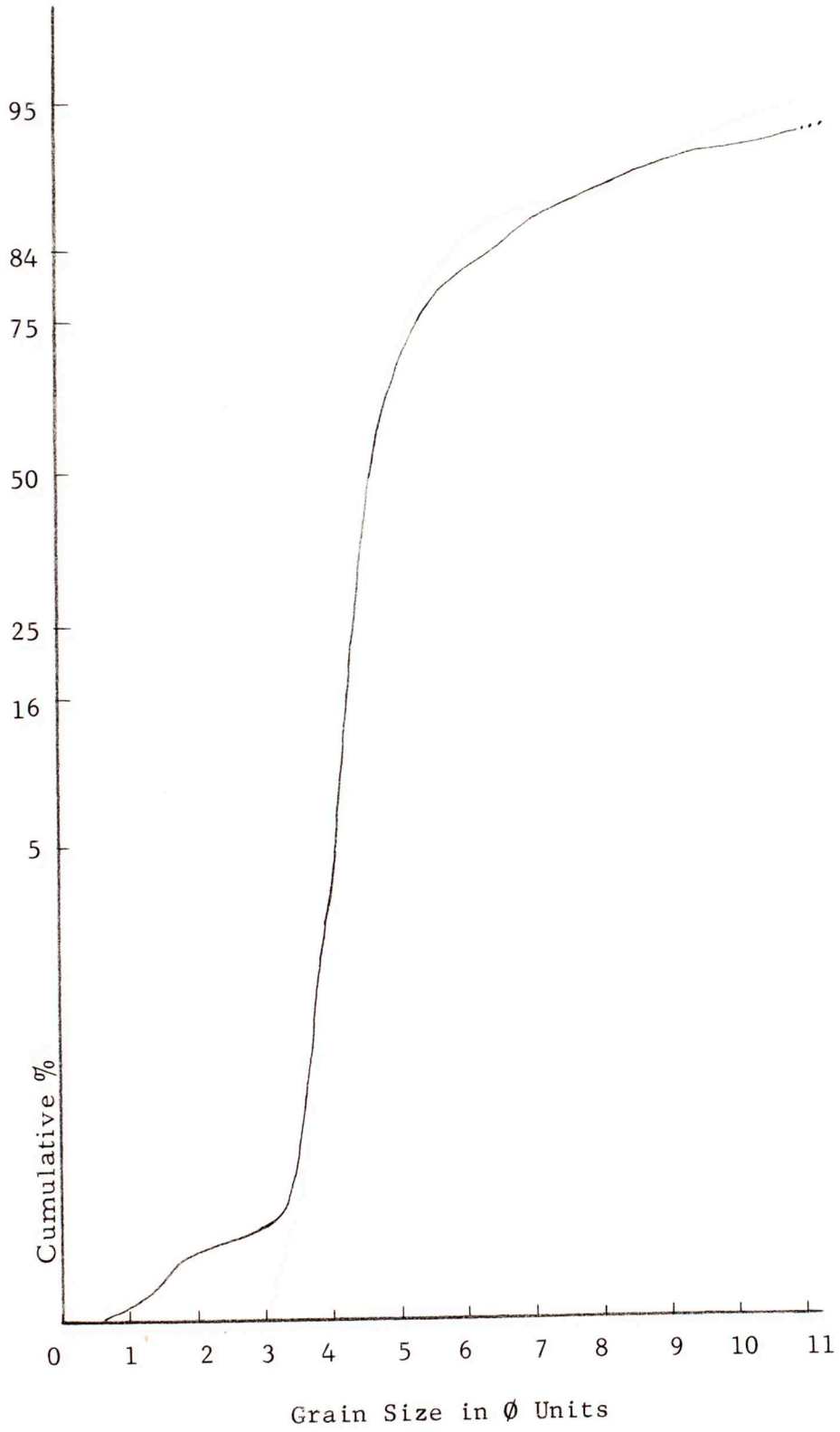

C-9-c

GRAIN-SIZE DISTRIBUTION, CUMULATIVE CURVE

Figure 11

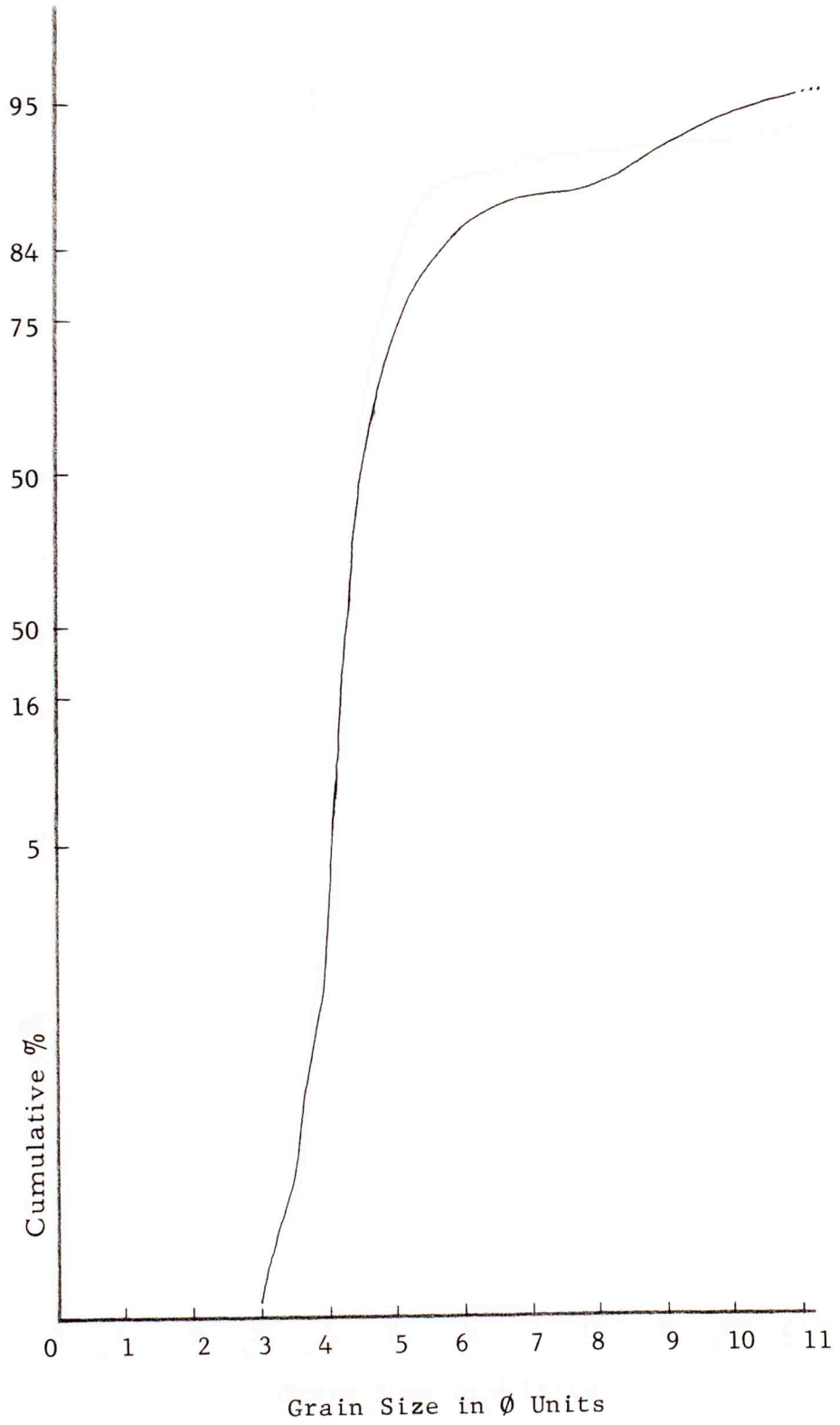

C-9-f

GRAIN-SIZE DISTRIBUTION, CUMULATIVE CURVE

Figure 12

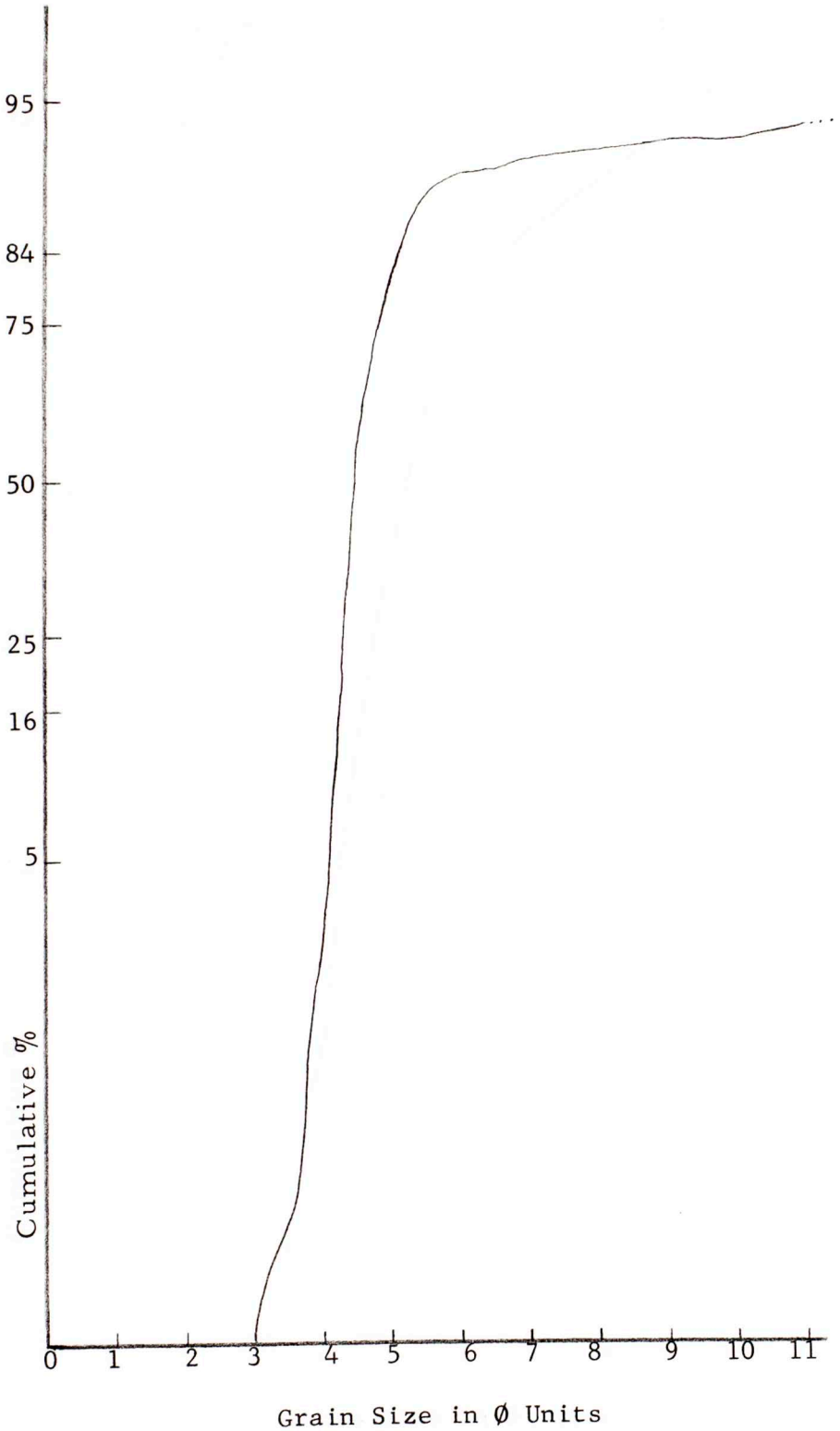

C-9-j

GRAIN-SIZE DISTRIBUTION, CUMULATIVE CURVE

Figure 13

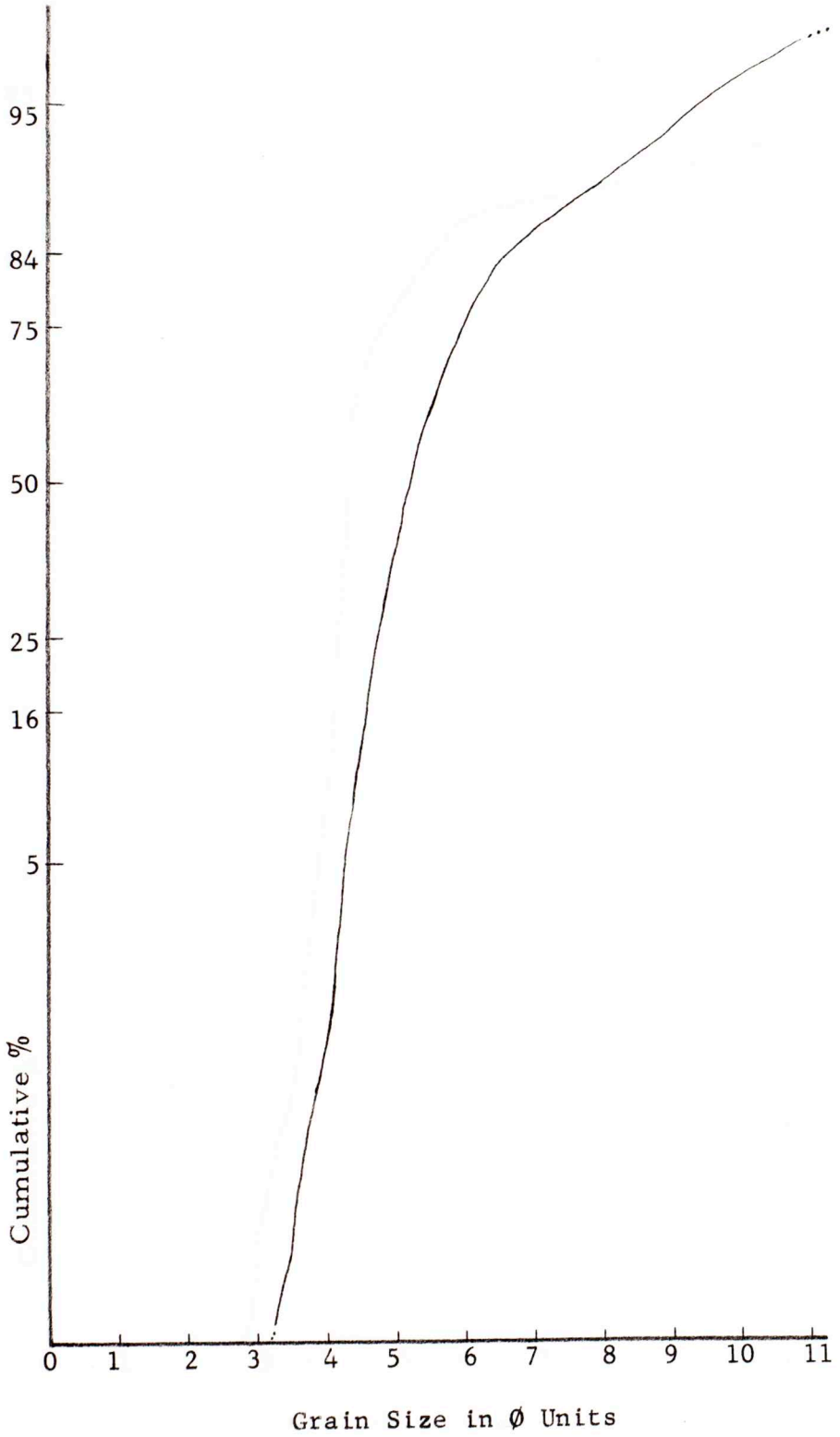

C-9-m

GRAIN-SIZE DISTRIBUTION, CUMULATIVE CURVE

Figure 14

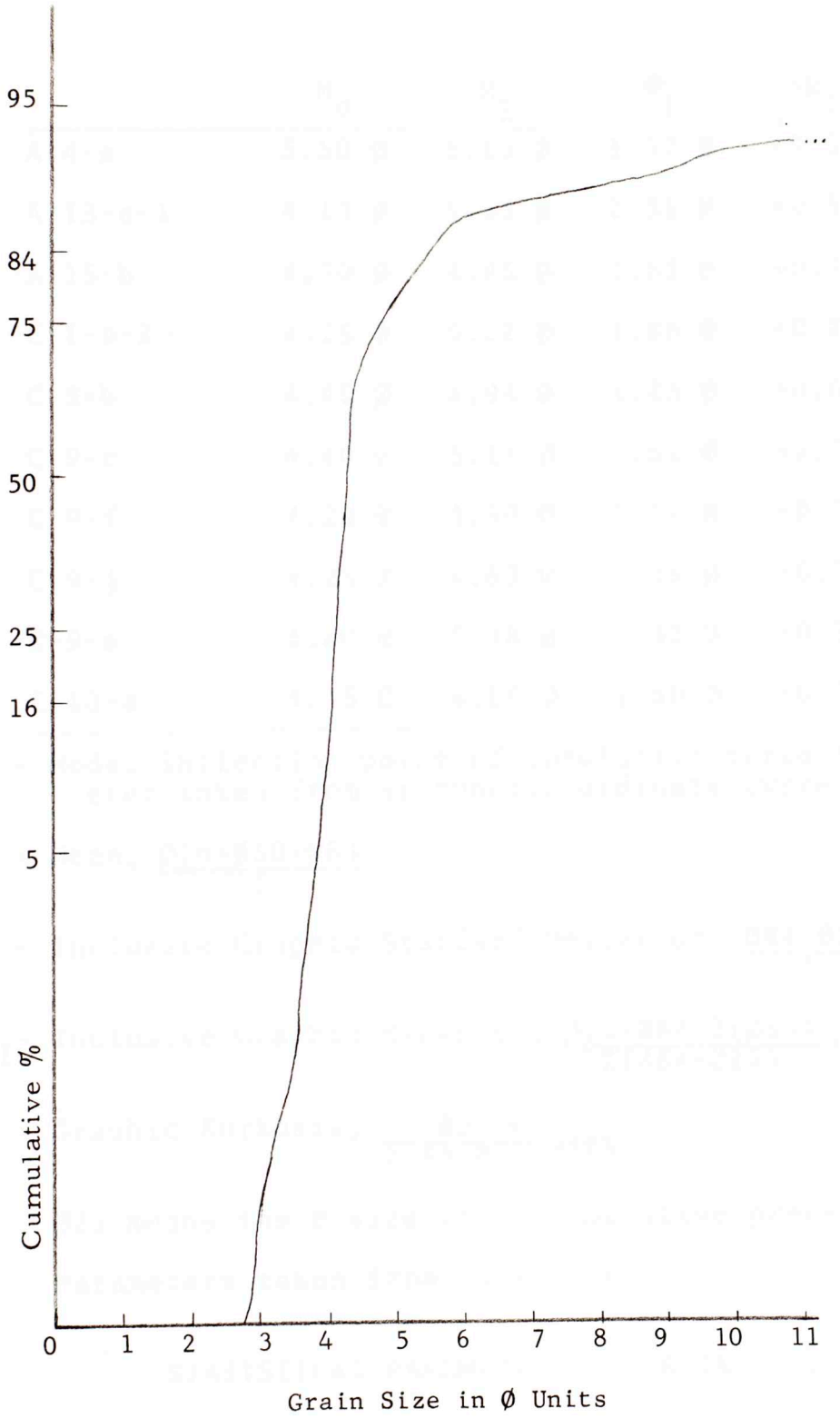

C-10-a

GRAIN-SIZE DISTRIBUTION, CUMULATIVE CURVE

Figure 15

	M_o	M_Z	σ_I	Sk_I	K_G
A-4-a	5.50 Ø	6.13 Ø	1.52 Ø	+0.59	2.39
A-13-e-1	4.13 Ø	5.63 Ø	2.31 Ø	+0.87	2.31
A-15-b	4.30 Ø	4.85 Ø	1.63 Ø	+0.77	3.94
C-1-a-2	4.25 Ø	5.22 Ø	1.86 Ø	+0.83	3.64
C-3-b	4.40 Ø	4.94 Ø	1.43 Ø	+0.63	3.35
C-9-c	4.40 Ø	5.11 Ø	1.62 Ø	+0.78	2.91
C-9-f	4.20 Ø	4.80 Ø	1.37 Ø	+0.73	3.36
C-9-j	4.25 Ø	4.60 Ø	1.28 Ø	+0.71	5.78
C-9-m	4.80 Ø	5.48 Ø	1.32 Ø	+0.50	1.72
C-10-a	4.15 Ø	4.65 Ø	1.50 Ø	+0.73	4.67

M_o - Mode, inflection point of cumulative curve (only parameter taken from arithmetic ordinate curve).

M_Z - Mean, $\frac{Ø16+Ø50+Ø84}{3}$

σ_I - Inclusive Graphic Standard Deviation, $\frac{Ø84-Ø16}{4} + \frac{Ø95-Ø5}{6.6}$

Sk_I - Inclusive Graphic Skewness, $\frac{Ø16+Ø84-2(Ø50)}{2(Ø84-Ø16)} + \frac{Ø5+Ø95-2(Ø50)}{2(Ø95-Ø5)}$

K_G - Graphic Kurtosis, $\frac{Ø95-Ø5}{2.44(Ø75-Ø25)}$

Ø25 means the Ø size at 25 cumulative precent point.

Parameters taken from Folk, 1961.

STATISTICAL PARAMETERS OF GRAIN SIZE

Table 4

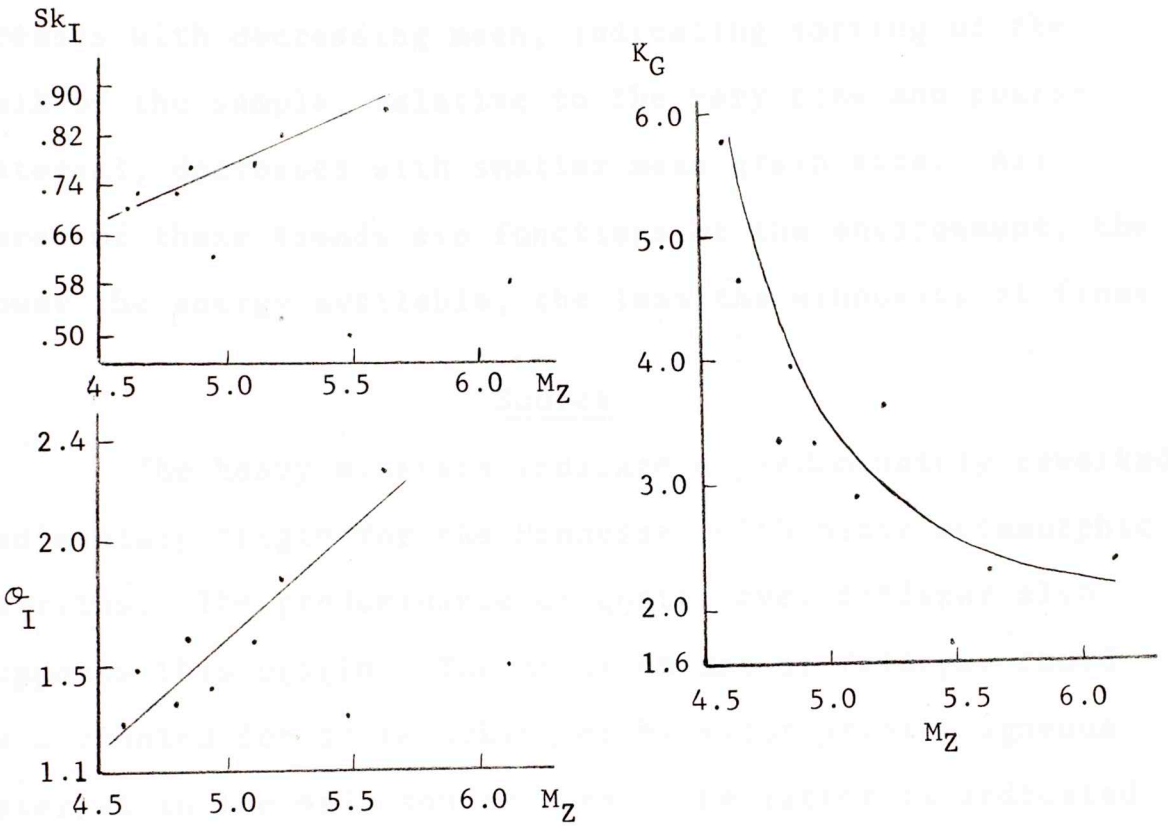

M_Z - Graphic Mean* *(Folk, 1961)

Sk_I - Inclusive Graphic Skewness*

K_G - Graphic Kurtosis*

σ_I - Inclusive Graphic Standard Deviation*

SCATTER DIAGRAMS

STATISTICAL PARAMETERS OF GRAIN SIZE

Figure 16

more poorly sorted than the coarser. Skewness increases with decreasing mean. This indicates the finer sediments have a greater excess of fine material. Also, kurtosis decreases with decreasing mean, indicating sorting of the bulk of the sample, relative to the very fine and coarse material, decreases with smaller mean grain size. All three of these trends are functions of the environment, the lower the energy available, the less the winnowing of fines.

Source

The heavy minerals indicate a predominately reworked sedimentary origin for the Hennessey with minor metamorphic detritus. The predominance of quartz over feldspar also supports this origin. The minor amount of feldspar could be accounted for by reworking or by minor primary igneous material in the main source area. The latter is indicated by the relative freshness of most of the feldspar grains and by the presence of euhedral zircon and subhedral to rounded apatite. The possibility of multiple sources is indicated by the somewhat anomalous alteration trends of the feldspar: large grains more altered than small, orthoclase more altered than plagioclase. Illite (primarily 2M polymorph) and chlorite (trioctahedral) indicate derivation from previous sedimentary rocks and metamorphic rocks rich in these two minerals. Most of the clay is probably detrital rather than authigenic. Minor to moderate amounts of

coarse, clastic chlorite indicate a metamorphic source.

The Hennessey grades into clastics and evaporites to the west (Nicholson, 1960) and to the northwest (Vosburg, 1964). To the south, its equivalents are shale and siltstones, and it is absent by erosion to the southeast. A review of the literature shows that the evaporites grade westward into arkosic deposits derived from the remnants of the "Ancestral Rockies" or Colorado Mountains (Cunningham, 1961; Eddleman, 1961; Oklahoma City Geological Society, 1956). With the intervening evaporite sequence, it is likely that little, if any, of the sediment in the thesis area was derived from Colorado and New Mexico.

The Wichita Mountains are not considered as a major source for several reasons. Arkosic material similar to the granites is found only in near-shore and channel facies and as isolated grains in trace amounts in the rest of the formation. Although metamorphic rocks (Tillman Metasedimentary Group) are found in the Wichita Province, they are below the present igneous exposures or are overlain by Cambrian sediments (Ham, Denison, and Merritt, 1964). Subcrop areas of Tillman that could have contributed to lower Permian sediments are extremely limited in size (Dr. W. E. Ham, personal communication, 1967). Current information indicates continuous deposition from the Wichita Formation to the Hennessey Shale with very little chance of reworking between formations. A special project by H. F. Alkersan

(personal communication, 1967) shows that the clay mineral suite of the Hennessey Shale in the vicinity of Norman, Oklahoma is identical to that in the Wichita Mountain area. This indicates the clay suite is uniform on both sides of the Anadarko Basin and not affected by contributions from the Wichita Mountains.

The Ouachita Structural Belt is a system of folded, faulted rocks that stretches from the southern end of the Appalachians westward to the Ouachita Mountains in Oklahoma and Arkansas, then south and west around the Llano uplift in Texas to the Marathon uplift, and then south into Mexico. Most of this is buried under the Cretaceous overlap. Surface and subsurface studies show abundant siltstone and sandstone; metamorphic rocks with incipient to low-grade facies; and the possibility of some Paleozoic acid igneous material. Clay minerals present in many of the formations are predominantly illite with minor to moderate amounts of chlorite. Metamorphic rocks include slate, phyllite, metaquartzite, and schist (Flawn, 1961; Goldstein, 1961; King, 1961; Weaver, 1961).

The Arbuckle and Ozark uplifts were other possible sources, but were probably low during Leonardian time and contributed little to the Hennessey (Flawn, 1961b). Rocks in these two areas are predominantly carbonate and shale with some acid igneous material which is not overly similar to the character of the Hennessey sediments.

Environment

The Hennessey Shale was deposited in a low-energy environment as shown by the sorting and fine grain size. Although ripple-marks, cross-bedding, channeling, and desiccation cracks (C-5-c) are present, they are scattered and minor. Some rocks show disruption by burrowing, but others are definitely intraclastic, indicating at least intermittantly higher energy in the depositional basin. The location of the series of siltstones in the western portion of the area indicates they are a function of environment rather than source. Nominal uplift of the Wichita-Amarillo trend could have created a slight ridge along an otherwise flat sea floor. Sediments accumulating along this trend would have a higher silt content than those in deeper water. The location of these siltstones is believed to be restricted to the axis of the Wichita-Amarillo trend (Dr. K. S. Johnson, personal communication, 1966). The climate was somewhat arid as shown by the evaporites to the west and northwest (Nicholson, 1960). Extreme weathering of the coarse clastic material could still be achieved in a semi-arid climate if the land surface was relatively low-lying as the Wichita Mountains were. The difference in alteration between the silt-sized feldspar and the coarse perthite indicates either an arid climate or high relief in the major source area and was probably due to high relief and rapid erosion.

The lamination of the beds and the skewness and kurtosis values of the siltstones indicate frequent and minor fluctuations in the energy of the environment or the sediment load, and probably both. Disaggregation of a rock composed of well sorted silt layers and clay layers will provide the leptokurtic, fine-skewed character noted for the Hennessey siltstones. Many of them show this lamination. Other causes for the difference in sorting between the clay and the bulk of the material are clay aggregates and clay coatings on coarser grains, both of which are noted in thin-section.

CONCLUSIONS

The Hennessey Shale is a series of marine siltstones, mudstones, and shales. The principle environment is shallow neritic with associated tidal-flat and near-shore facies. The bulk of the rocks are orthoquartzites, mudstones, and claystones with some subgraywacke, subarkose, and carbonate beds. The major cement is dolomite, penecontemporaneously altered from calcite.

No further answers were provided for the question of the origin of red coloration in shales. Indications are that some of it is post-depositional. Field studies show many of the green reduction spots and zones are associated with carbonaceous spots and fractures, but many have no such clear origin. It does seem, however, that there is no difference whatsoever in the red and green sediment other than the reduction of the iron oxide.

Mineralogy of both the light and heavy fractions indicate a source area composed of terrigenous sedimentary rocks with minor acid plutonic, metamorphic, and pegmatitic rocks. The contribution of the Wichita Mountains is shown to be minor in all facies except the near-shore and channel

facies. Lithology, intervening sediment types, and structural considerations eliminate the Colorado Mountains, Arbuckle Uplift, and Ozark Uplift as source areas for more than minor contributions of sediment. The Hennessey is low in arkosic material and separated from the Colorado Mountains by evaporites. The sedimentary rocks in the Arbuckle Uplift are mainly carbonate with minor shale. This shale contains illite but does not have chlorite. The lower Paleozoic rocks of the Ozark Uplift have a clay mineral suite high in kaolinite (Dr. C. J. Mankin, personal communication, 1967) which is not found in the Hennessey. The Ouachita System is low in carbonate rocks, high in terrigenous and metamorphic rocks, and has abundant chlorite and illite. The absence of kaolinite and abundant carbonate rock fragments; presence of illite, chlorite, and metamorphic detritus; and grain size of the Hennessey indicate a moderately distant source area with a varied composition as would be provided by the Ouachita Structural Belt.

An intermittantly unconformable contact between the Hennessey and Duncan, mentioned by previous writers, is strengthened by the demonstrated alterations in mineralogy in the upper portion of the Hennessey.

Clay mineralogy of the formation is uniform. Illite is the major clay with chlorite being present in trace to moderate amounts. The illite-chlorite mechanical mixture at the base of the formation shows a marked similarity to

the underlying Wichita Formation. Crystallinity of the core samples in all cases is just slightly better than the surface samples. This variation is attributed to present day surface weathering. The alteration of chlorite to randomly interlayered chlorite-vermiculite increases from east to west. This alteration proceeds by removal of iron and probably magnesium from the brucite layer and is more pronounced in the finer than in the coarser fractions. The alteration is present in both core and surface samples and is therefore not due to present day surface weathering. An increase in fluid circulation due to increasing silt content in the western portion of the area is a probable cause of the alteration.

SELECTED REFERENCES

Aurin, F. L., Officer, H. G., and Gould, C. N., 1926, The subdivision of the Enid Formation: Amer. Assoc. Petroleum Geologists, Bull., v. 10, pp. 786-799.

Becker, C. M., 1930, Structure and stratigraphy of southwestern Oklahoma: Amer. Assoc. Petroleum Geologists, Bull., v. 14, pp. 37-55.

Biscaye, P. E., 1964, Distinction between kaolinite and chlorite in recent sediments by x-ray diffraction: Amer. Mineralogist, v. 49, pp. 1281-1289.

Bradley, W. F., and Weaver, C. E., 1956, A regularly interstratified chlorite-vermiculite clay mineral: Amer. Mineralogist, v. 41, pp. 497-504.

Brophy, G. P., and Sheridan, M. F., 1965, Sulfate studies IV: The jarosite-natrojarosite-hydronium jarosite solid solution series: Amer. Mineralogist, v. 50, pp. 1595-1607.

Brown, G., Editor, 1961, The X-ray Identification and Crystal Structure of Clay Minerals (Symposium): London, Mineralog. Soc. (Clay Minerals Group), 544 p.

Cunningham, B. J., 1961, Stratigraphy Oklahoma-Texas panhandles, pp. 45-60, in Oil and Gas Fields of the Texas and Oklahoma Panhandles (Symposium): Panhandle Geological Society.

Eddleman, M. W., 1961, Tectonics and geologic history of the Texas and Oklahoma panhandles, pp. 61-68, in Oil and Gas Fields of the Texas and Oklahoma Panhandles (Symposium): Panhandle Geological Society.

Everett, A. G., 1962, Clay Petrology and Geochemistry of the Blaine Formation (Permian), Northern Blaine County, Oklahoma: Unpublished M. S. Thesis, University of Oklahoma.

Flawn, P. T., 1961a, The subsurface Ouachita Structural Belt in Texas and southeast Oklahoma, pp. 65-82, in The Ouachita System: Bur. of Econ. Geol., University of Texas, pub. no. 6120.

_____, 1961b, Igneous and vein rocks in the Ouachita Belt, pp. 107-119 in The Ouachita System: Bur. of Econ. Geol., University of Texas, pub. no. 6120.

_____, 1961c, Metamorphism in the Ouachita Belt, pp. 121-124, in The Ouachita System: Bur. of Econ. Geol., University of Texas, pub. no. 6120.

_____, 1961d, Foreland basin and shelf rocks north and west of the Ouachita Structural Belt, pp. 129-146, in The Ouachita System: Bur. of Econ. Geol., University of Texas, pub. no. 6120.

Folk, R. L., 1961, Petrology of Sedimentary Rocks: Austin, Hemphill's, 154 p.

Goldstein, A. G., 1961, The Ouachita Mountains of Oklahoma and Arkansas, pp. 21-48, in The Ouachita System: Bur. of Econ. Geol., University of Texas, pub. no. 6120.

Gould, C. N., 1905, Geology and Water Resources of Oklahoma: U. S. Geol. Survey Water-Supply and Irrigation Paper 148, pp. 34-44.

_____, 1923, Crystalline rocks of the plains: Geol. Soc. America, Bull., v. 34, pp. 551-552.

_____, 1924, A new classification of the Permian redbeds of southwestern Oklahoma: Amer. Assoc. Petroleum Geologists, Bull., v. 8, pp. 322-341.

_____, and Lewis, F. E., 1926, The Permian of Western Oklahoma and the Panhandle of Texas: Okla. Geol. Survey, Circ. no. 13, 29 p.

Grim, R. E., 1951, The depositional environment of red and green shales: Jour. Sed. Petrology, v. 21, pp. 226-232.

_____, 1953, Clay Mineralogy: New York, McGraw-Hill Book Co., Inc., 384 p.

_____, and Johns, W. D., 1953, Clay mineral investigation of sediments in the northern Gulf of Mexico, pp. 81-103, in Clays and Clay Minerals: Nat. Acad. of Sciences-Nat. Res. Council, pub. no. 327.

Ham, W. E., Denison, R. E., and Merritt, C. A., 1964, Basement Rocks and Structural Evolution of Southern Oklahoma: Okla. Geol. Survey, Bull. 95, 302 p.

Ham, W. E., and Merritt, C. A., 1944, Barite in Oklahoma: Okla. Geol. Survey, Circ. no. 23, 42 p.

Hathaway, J. C., 1955, Studies of some vermiculite-type clay minerals, pp. 74-86, in Clays and Clay Minerals: Nat. Acad. of Sciences-Nat. Res. Council, pub. no. 395.

Hey, M. H., 1954, A new review of the chlorites: Min. Magazine, v. 30, pp. 277-292.

Huffman, G. G., 1958, Geology of the Flanks of the Ozark Uplift, Northeastern Oklahoma: Okla. Geol. Survey, Bull. 77, 281 p.

Hunt, D. G., 1963, Clay Mineralogy of the Vermejo Formation (Upper Cretaceous), Canon City, Colorado: Unpublished M. S. Thesis, University of Oklahoma.

Johns, W. D., and Grim, R. E., 1958, Clay mineral composition of Recent sediments from the Mississippi River delta: Jour. of Sed. Petrology, v. 28, pp. 186-199.

Johnson, K. S., 1962, Areal Geology of the Sentinel-Gotebo Area, Kiowa and Washita Counties, Oklahoma: Unpublished M. S. Thesis, University of Oklahoma.

Jonas, E. C., and Roberson, H. E., 1960, Particle size as a factor influencing expansion of the three-layer clay minerals: Amer. Mineralogist, v. 45, pp. 828-838.

Kerr, P. F., 1959, Optical Mineralogy: 3rd. ed., New York, McGraw-Hill Book Co., Inc., 442 p.

King, P. B., 1961, History of the Ouachita System, pp. 175-190, in The Ouachita System: Bur. of Econ. Geol., University of Texas, pub. no. 6120.

Krynine, P. D., 1946, The tourmaline group in sediments: Jour. Geol., v. 54, pp. 65-87.

Martin, R. T., 1955, Reference chlorite characterization for chlorite identification in soil clays, pp. 117-145, in Clays and Clay Minerals: Nat. Acad. of Sciences-Nat. Res. Council, pub. no. 395.

Melton, F. A., 1930, Age of the Ouachita Orogeny and its tectonic effects: Amer. Assoc. Petroleum Geologists, Bull., v. 14, pp. 57-72.

Merritt, C. A., 1958, Igneous Geology of the Lake Altus Area, Oklahoma: Okla. Geol. Survey, Bull. 76, 70 p.

Milner, H. B., 1952, Sedimentary Petrography: 3rd. ed., London, Thomas Murby and Co., 666 p.

Miser, H. D., 1954, Geologic Map of Oklahoma: Okla. Geol. Survey and U. S. Geol. Survey, scale 1:500,000.

Nicholson, J. H., 1960, Geology of the Texas panhandle, pp. 51-64, in Aspects of the Geology of Texas (Symposium): Bur. of Econ. Geol., University of Texas, pub. no. 6017.

Oklahoma City Geological Society, 1956, 35th Anniversary Field Conference, Oklahoma Panhandle, Northeastern New Mexico, and South-Central Colorado, 189 p.

Permian Subcommittee of the National Research Council's Committee on Stratigraphy, 1960, Correlation of the Permian formations of North America: Geol. Soc. America, Bull., v. 71, pp. 1763-1806.

Pettijohn, F. J., 1957, Sedimentary Rocks: 2nd ed., New York, Harper and Brothers, 718 p.

Sawyer, R. W., 1924, Areal geology of a part of southwestern Oklahoma: Amer. Assoc. Petroleum Geologists, Bull., v. 8, pp. 312-321.

———, 1929, Oil and Gas in Oklahoma, Kiowa and Washita Counties: Okla. Geol. Survey, Bull. no. 40-HH, pp. 9-10.

Schweer, H., 1937, Discussion of: Unconformity at base of Whitehorse Formation, Oklahoma (Brown, O. E.): Amer. Assoc. Petroleum Geologists, Bull., v. 21, pp. 1554-1555.

Scott, G. L., Jr., 1955, Areal Geology of Portions of Beckham, Greer, Kiowa, and Washita Counties, Oklahoma: Unpublished M. S. Thesis, University of Oklahoma.

Self, R. P., 1966, Petrology of the Duncan Sandstone (Permian) of South-Central Oklahoma: Unpublished M. S. Thesis, University of Oklahoma.

Shirozu, H., 1958, X-ray powder patterns and cell dimensions of some chlorites in Japan, with a note on their interference colors: Mineralogical Jour., v. 2, pp. 209-223.

Temple, A. K., 1966, Alteration of ilmenite: Econ. Geology, v. 61, pp. 695-714.

Tyler, S. A., and Marsden, R. W., 1938, The nature of leucoxene: Jour. of Sed. Petrology, v. 8, pp. 55-58.

Vosburg, D. L., 1963, Permian Subsurface Evaporites in the Anadarko Basin of the Western Oklahoma-Texas Panhandle Region: Unpublished Ph. D. Dissertation, University of Oklahoma.

Weaver, C. E., 1956, The distribution and identification of mixed-layer clays in sedimentary rocks: Amer. Mineralogist, v. 41, pp. 202-221.

_____, 1958a, The effects and geologic significance of potassium "fixation" by expandable clay minerals derived from muscovite, biotite, chlorite, and volcanic material: Amer. Mineralogist, v. 43, pp. 839-861.

_____, 1958b, A discussion of the origin of clay minerals in sedimentary rocks, pp. 159-173, in Clays and Clay Minerals: Nat. Acad. of Sciences-Nat. Res. Council, pub. no. 566.

_____, 1959, The clay petrology of sediments, pp. 154-187, in Clays and Clay Minerals, Proceedings of the 6th National Conference on Clays and Clay Minerals: London, Pergamon Press.

_____, 1961, Clay minerals of the Ouachita Structural Belt and adjacent foreland, pp. 147-162, in The Ouachita System: Bur. Econ. Geol., University of Texas, pub. no. 6120.

Weiss, E. J., and Rowland, R. A., 1956a, Oscillating-heating x-ray diffractometer studies of clay mineral dehydroxylation: Amer. Mineralogist, v. 41, pp. 117-126.

_____, 1956b, Effect of heat on vermiculite and mixed-layer vermiculite-chlorite: Amer. Mineralogist, v. 41, pp. 899-914.

Yoder, H. S., and Eugster, H. P., 1955, Synthetic and natural muscovites: Geochim. et Cosmochim. Acta, v. 8, pp. 225-280.

APPENDIX I

Analytical Techniques

Sample Preparation

Each sample was ground to less than 80 mesh with a ceramic mortar and pestle. Splits were then obtained of approximately 10 grams and 70 grams. The larger split was stored in a glass bottle against future needs. The smaller split was placed in a beaker filled with distilled water and dispersed in an autosonic generator. Calgon was added as a dispersant to all samples at the rate of 2.54 grams per liter of water.

Oriented slides for x-ray diffraction were prepared from the dispersed sample. Withdrawal from 1 centimeter after a 15 minute wait was the technique used to obtain material of less than 4 microns equivalent spherical diameter. Randomly oriented powder slides were made by crushing the sample to less than 115 mesh and sieving the material directly onto a vaseline-coated slide.

Oriented slides were first placed in a constant humidity environment, approximately 50 percent relative humidity, for a minimum of 8 hours before being x-rayed. The

slides were then placed in an ethylene glycol atmosphere at 60°C for a minimum of 8 hours and x-rayed again.

Size Fractionation

Particle size fractionation was done partly by decantation and partly by continuous-flow centrifuge. Settling to 20 centimeters for 3.5 hours produced the less than 4 microns and repeated settling to 10 centimeters for 24 hours produced the less than 1 micron size. The remaining size fractions were obtained by continuous-flow centrifuging: ½-1 micron, flow rate of 5 minutes per liter, centrifuge speed 3,000 RPM; ¼-½ micron, 5 minutes per liter at 6,000 RPM; and 1/8-¼ micron, 5 minutes per liter at 12,000 RPM.

X-ray Diffraction

The equipment used consisted of a Norelco generator, goniometer, scintillation counter, and recorder and a similarly equipped Siemens generator. Nickel-filtered copper K-α radiation was used in both generators. Five samples were examined on a Norelco goniometer equipped with a high-temperature, beryllium-window furnace which permitted continuous recording of x-ray diffraction during heating from room temperature to 1000°C. The furnace programmer also allowed interruption of the heating cycle and maintenance of any given temperature for a period of the time before resuming heating.

Powder patterns were run from 5° to 60-65° 2θ,

oriented-humidified slides from 2-3° to 46° 2θ, and oriented-ethylene glycol slides were run for a variable distance, determined by the mineralogy present.

Differential Thermal Analysis

Samples were run on a Robert L. Stone Model DTA-13M differential thermal analysis unit using an inconel sample holder, helium as a purging gas, and a heating rate of 10°C per minute. The samples run were dried powder, ground to less than 80 mesh. The purging gas was maintained at constant pressure. Care was taken to insure that the quantity of material used and the degree of packing of the sample were constant.

Particle Size Distribution Analysis

Siltstone samples were analyzed by sieve and pipette techniques. The samples were initially disaggregated by gentle crushing in a mortar and pestle. Two samples were weathered and friable enough that this was sufficient. The remaining samples were treated with warm HCl for 8 hours to remove the carbonate cement. Sand distribution was determined by using a U. S. Standard Sieve set with a ¼ Ø-unit interval. Each sample was agitated for 15 minutes on a Ro-Tap machine and the size fractions weighed.

The material less than 4 Ø, silt and clay, was weighed and dispersed in a liter of distilled water. Periodic withdrawals of 20 milliliters of the suspension were then

made at the following times and depths:

4.0 Ø	20 cm		20 sec
4.5 Ø	20 cm	1 min	45 sec
5.0 Ø	20 cm	3 min	30 sec
5.5 Ø	15 cm	5 min	10 sec
6.0 Ø	10 cm	7 min	
6.5 Ø	10 cm	14 min	20 sec
7.0 Ø	10 cm		28 min
8.0 Ø	10 cm	1 hr	40 min
9.0 Ø	5 cm	3 hr	25 min
10.0 Ø	2.5 cm	6 hr	40 min
11.0 Ø	1.2 cm	13 hr	20 min

Temperature of the laboratory was 26-27°C. Times and depths of the withdrawals were determined from a nomograph in use at the University of Oklahoma, derived from Stokes' Law. The withdrawals were placed in dry, weighed beakers and dried at 70°C, cooled for 4 hours to insure adjustment to atmospheric conditions, and weighed. Computation of the cumulative percent of each size was then done by the method of Folk (1961). The results of the sieve and pipette analysis for each sample were combined into a cumulative curve drawn on probability paper. Various statistical measures (Folk, 1961) were then completed for each sample.

Heavy Mineral Separation

Due to the grain size of the samples and the mesh of the available sieves, heavy minerals were separated from the 4.0-4.75 Ø fraction of the siltstones. Separation was done using an International Centrifuge, model C50 and tetrabromoethane. Samples were run at approximately 4,000 RPM for 5-10 minutes, stirred, and run again. The lights were

poured from the top of the centrifuge tubes and the heavies washed from the bottom. After drying, the heavy mineral crop was separated into two more or less equal fractions, magnetic and non-magnetic, on a Frantz Isodynamic Separator.

Grain mounts were then made of each sample in Lakeside 70 C and identified on a Leitz petrographic microscope. X-rays were run on several of the samples as an aid in identification. Percentages were determined by counting 300 grains in each slide.

Sampling

Outcrops were selected to give the best possible coverage of the formation. Each outcrop was measured and divided into beds by variation in lithology and color. Samples were then taken from the main variations at each outcrop. Both vertical and horizontal variations were sampled. One to two liters of each sample were placed in cloth sample bags. Depth of sampling was surface to 1 foot deep, depending on weathering conditions.

Each of the three sample areas (see Methods of Investigation) are designated by a capital letter, A, B, C. Each outcrop in the traverse is then designated by a number, A-13, B-5, etc. The different beds at each outcrop are then designated by lower-case letters, A-13-p, B-5-a, etc. Finally, if more than one sample per bed is taken, each is designated by another number. The final sample designation would

then be: Line, Outcrop, Bed, Sample; A-13-p-5.

Petrographic thin-sections furnished by the University of Oklahoma are numbered 964 to 979. Those prepared by the writer are not numbered.

APPENDIX II

Sample Locations

Outcrop	Location
A-1	Cen. E½ NW¼ sec. 36, T. 6 N., R. 18 W.
A-2	Cen. N½ SW¼ NE¼ sec. 25, T. 6 N., R. 18 W.
A-3	NE¼ NW¼ NE¼ SE¼ sec. 19, T. 6 N., R. 17 W.
A-4	Cen. W line SW¼ NW¼ sec. 20, T. 6 N., R. 17 W.
A-5	Cen. N½ NE¼ NW¼ NW¼ sec. 20, T. 6 N., R. 17 W.
A-6	Cen. N line NW¼ NW¼ sec. 17, T. 6 N., R. 17 W.
A-7	Cen. S½ SW¼ sec. 8, T. 6 N., R. 17 W.
A-8	Cen. E line NE¼ SE¼ NE¼ sec. 8, T. 6 N., R. 17 W.
A-9	NW¼ NW¼ NE¼ sec. 9, T. 6 N., R. 17 W.
A-10	Cen. W½ NW¼ sec. 4, T. 6 N., R. 17 W.
A-11	Cen. N line NW¼ NW¼ NW¼ sec. 33, T. 7 N., R. 17 W.
A-12	On S line 1200' from E line sec. 27, T. 7 N., R. 17 W.
A-13	From base at NE¼ SW¼ NE¼ sec. 27, T. 7 N., R. 17 W. northwest to top in escarpment in N½ SW¼ SW¼ SE¼ sec. 22, T. 7 N., R. 17 W.
A-14	Cen. E½ NW¼ NW¼ sec. 26, T. 7 N., R. 17 W.
A-15	SE¼ NW¼ SW¼ sec. 23, T. 7 N., R. 17 W.
A-17	Cen. W½ NE¼ sec. 18, T. 7 N., R. 16 W.
A-18	SE¼ SE¼ sec. 8, T. 7 N., R. 16 W.
A-19	NE¼ NE¼ sec. 9, T. 7 N., R. 16 W.
20	Cen. W½ sec. 33, T. 7 N., R. 20 W.
21	Cen. N line SE¼ sec. 27, T. 5 N., R. 20 W.
A-22	Cen. NW¼ sec. 11, T. 7 N., R. 16 W.
B-1	Cen. N½ SW¼ NE¼ sec. 10, T. 5 N., R. 19 W.
B-2	NE¼ SE¼ NW¼ SW¼ sec. 9, T. 5 N., R. 19 W.
B-3	Cen. S½ SE¼ SE¼ sec. 5, T. 5 N., R. 19 W.
B-4	SE¼ NE¼ sec. 5, T. 5 N., R. 19 W.
B-5	N½ S½ S½ sec. 32, T. 6 N., R. 19 W.
B-6	Cen. S½ NW¼ sec. 32, T. 6 N., R. 19 W.
B-7	SE¼ SW¼ SW¼ SW¼ sec. 13, T. 6 N., R. 19 W.
B-8	Cen. E½ W½ NW¼ sec. 24, T. 6 N., R. 19 W.
B-9	NE¼ NW¼ SE¼ SW¼ sec. 24, T. 6 N., R. 19 W.
B-10	Cen. S line, sec. 24, T. 6 N., R. 19 W.
B-11	NE corner sec. 36, T. 7 N., R. 19 W.
B-12	On cen. line 375' E of W line sec. 30, T. 7 N., R. 18 W.
C-1	Cen. W½ W½ sec. 20, T. 6 N., R. 22 W.

C-2	Cen. NE¼ SE¼ sec. 29, T. 6 N., R. 22 W.
C-3	From cen. N½ SE¼ SE¼ sec. 29, T. 6 N., R. 22 W. southwest along escarpment to S line sec. 29.
C-4	From NW¼ SE¼ NE¼ sec. 32, T. 6 N., R. 22 W. southwest to river.
C-5	On north bank of river approximately 0.1 mile W of dam/road in SE¼ sec. 21, T. 5 N., R. 20 W.
C-6	Cen. E½ SE¼ SE¼ sec. 19, T. 5 N., R. 20 W.
C-7	150' S of cen. N line sec. 34, T. 6 N., R. 21 W.
C-8	Cen. S½ SE¼ SW¼ sec. 21, T. 6 N., R. 21 W.
C-9	From NE corner sec. 19, T. 6 N., R. 21 W. west to cen. NW¼ NE¼ NE¼ NW¼ same section.
C-10	From 1600' east of NW corner west to NW corner sec. 24, T. 6 N., R. 22 W.
C-11	Cen. NW¼ NE¼ NE¼ sec. 2, T. 6 N., R. 22 W.

Corehole	Location
AL-1	Cen. NE¼ sec. 13, T. 7 N., R. 16 W.
AL-2	NW¼ sec. 13, T. 6 N., R. 19 W.
Gotebo	NE¼ SW¼ SW¼ sec. 2, T. 7 N., R. 16 W.
Granite	NW¼ sec. 33, T. 6 N., R. 21 W.

APPENDIX III

Measured Sections

Sample		Feet
I.	Section measured at outcrop A-13.	
A-13-		
p-	Shale, green to tan, with intermittant silty and limonite-stained beds, upper 11 feet browner than lower 8.5 feet.	19.5
7	tan shale, 18' below top.	
1	green shale, silty, resistant, 17' below top.	
2	green shale, 11.5' below top.	
3	limonite-stained zone, 8" thick, 11' below top.	
4	brown shale, 5' below top.	
5	limonite-stained zone, 3' below top.	
6	tan shale, malachite-stained, 6" thick, 1' below top.	
o-	Shale, red with green spots, some interbedded green shale, slightly blocky.	16.3
3	dark red shale, few green spots, 8.5' thick, 7' below top.	
2	green shale, 9" thick, 8.5' below top.	
1	dark red shale, few green spots, 5' thick, 12.8' below top.	
	Shale, green silty.	0.7
	Shale, red, silty.	0.7
n	Siltstone, gray-green, calcareous, platy.	0.6
m-	Shale, dark red with some green mottling, green spots, silty in places.	10.5
2	dark red shale with few green spots, 4' thick, 4.5' below top.	
1	dark red shale, weathers dark, 1.5' thick, 9.5' below top.	

k	Shale, interbedded green and red, silty, black concretions in base, 1.5' below top.	2.2
j-	Shale, red, green spots, silty zones.	10.0
2	shale, light red, numerous green spots, silty, 2" thick, 1' below top.	
1	shale, red, 5.5' below top.	
	Covered	
1-	Shale, red interbedded with gray-green, few green spots in upper half.	9.0
1	green shale, 1' thick, 2' below top.	
2	dark red shale, 7' below top.	
i	Shale, dark red, sampled in middle.	1.5
h	Claystone, green, noncalcareous.	1.0
	Covered	
f	Siltstone, light gray-green, noncalcareous, thin-bedded, very friable.	1.0
e-	Siltstone, light gray to tan, medium-grained, calcareous, beds paper thin to 2" thick, lower 3" slightly sandy, upper and lower thirds more resistant than middle.	1.5
3	upper third of unit.	
2	middle third, very friable.	
1	lower third, resistant, 1mm rounded grains of pink barite.	
d	Shale, mottled tan and green, intermittant limonite zones, 2.7' below top.	5.9
c	Shale, gray-green, noncalcareous, 1.5' below top.	4.0
	Covered	
II.	Compound section measured from top in outcrop C-1 to base in outcrop C-4.	
C-1-		
a-	Siltstone, light gray, calcareous, friable, no apparent bedding, rounded grains of quartz and pink feldspar in basal 2", top eroded. "Brinkman Bed"	6.0
2	2.5' below top.	
1	basal 2".	

b	Shale, red, silty, 7.3' below top.	9.5
c	Siltstone, light gray, thin-bedded.	0.6
	Shale, green, highly weathered.	1.0
d	Shale, red, highly weathered, sampled in middle.	2.0
e	Siltstone, light gray, beds up to 2" thick.	0.5
	Shale, gray, poorly exposed.	0.5
f	Shale, red-brown.	2.0
C-2-		
a-	Alternating siltstone and silty shale, gray-green and red, thin-bedded, Bed "Z".	12.0
	siltstone, red and green, irregular to thin-bedded, 0.8' thick	
1	shale, upper 2/3 red, lower 1/3 green, 2' thick, sampled 1' below top.	
2	siltstone, light gray, irregular to thin-bedded, 1.5' thick, sampled at top.	
3	siltstone, gray, friable, 1' thick.	
	hale, green, 6" thick.	
	siltstone, light gray and red, irregular to massive-bedded, 2" thick. Base of Bed "Z".	
C-3-		
a-	Shale, red with some green mottling in upper 5'.	18.0
1	1' below top.	
2	11' below top.	
b	Siltstone, light gray-green, coarse-grained, calcareous, thin-bedded, some channeling in middle, sampled in channel. Bed "Y".	1.0
c	Shale, green.	0.3
d	Shale, red, 7' below top.	9.0
e	Siltstone, gray, thin-bedded with shale interbeddings.	1.0
f-	Shale, red, thin gypsum seams, several to the inch, in the lower and upper thirds.	8.0
1	1.5' below top, contains gypsum.	
2	3.5' below top, no gypsum.	

g	Siltstone, light gray, sandy, numerous gypsum stringers, thin-bedded, top and base gradational into shale, variable thickness, sampled 4' below top. Bed "X".	4.0-6.0
C-4-		
a-	Shale, upper ½ red, lower ½ green, silty.	3.0
1	red shale, 1' below top.	
2	green shale, 2' below top.	
b-	Shale, red, gypsum veins and seams up to 2" thick.	34.0
1	red shale, 6' below top.	
2	red shale, 17' below top.	
3	green shale zone, 22' below top.	
4	red shale, 29' below top.	
c-	Siltstone, light gray, numerous selenite seams and red gypsum concretions, friable, appears massive. Bed "W".	5.3
1	siltstone, 3.5' below top.	
2	siltstone, 4.7' below top.	
3	red gypsum concretions.	
d	Shale, green.	0.3
e	Shale, red, numerous gypsum seams.	3.0
III.	Compound section measured from top in outcrop C-10 to base in outcrop C-9.	
C-10-		
a	Siltstone, light gray, calcareous, friable, coarse-grained, no apparent bedding, rounded grains of quartz and pink feldspar in lower part, top eroded, sampled 3.5' below top. "Brinkman Bed".	6.0
b	Shale, red, highly weathered, 2' below top.	4.0
	Siltstone, gray, interbedded with shale, friable.	2.0
	Shale, red, poorly exposed.	10.0
c	Siltstone, light gray, micaceous, interbedded with shale, friable, 4.5' below top.	6.0
d	Shale, gray-green, silty.	0.5
e	Claystone, red, 1.5' below top.	6.0

C-9-		
m	Siltstone, light gray, calcareous, medium-grained, thin-bedded to beds 4" thick, sampled in middle. Base of Bed "Z".	2.0
l	Shale, green, sampled in middle.	2.0
k	Shale, red, 6' below top.	12.0
j	Siltstone, light-gray, calcareous, coarse-grained, cross-bedded, ripple-marked, upper 3" non-laminated. Bed "Y".	2.0
i-	Shale and claystone, green, persistant yellowish-tan zone in middle.	1.3
2	yellowish-tan shale.	
1	basal green shale.	
h	Shale, red, sampled 1.5' below top.	6.0
	Siltstone, interbedded with shale, light gray and red.	1.0
	Shale, red.	2.0
g	Shale, yellow-green, sampled 2' below top.	3.0
f	Siltstone, light tan to gray, calcareous, coarse-grained, thin-bedded, sampled 3' below top. Bed "X".	4.0
	Siltstone, green-gray, shaly.	2.5
e	Shale and claystone, green, sampled ½' below top.	3.0
d-	Shale, red.	23.0
2	green shale zone, 1' thick, sampled 8.5' below top.	
1	red shale, sampled 10' below top.	
c	Siltstone, light gray-green, calcareous, medium-grained, some angular quartz and feldspar, thin-bedded, sampled basal 4". Bed "W".	3.0
	Shale, green-gray.	5.5
b-	Shale and claystone, red.	9.0
1	red shale, sampled 2.5' below top.	

2	red claystone, some angular quartz and feldspar, sampled 4' below top.	
	Shale, green-gray.	1.0
	Siltstone, light gray, thin-bedded.	1.0
a	Shale and claystone, green, few angular quartz and feldspar grains, variable thickness.	0.5-1.0
	Shale, red.	2.0

APPENDIX IV

Thin-section Description

Terminology is taken from Folk (1961). Descriptions of terrigenous rocks follow the outline below. Carbonates are modified from the outline given.

Thin-section # (if numbered)

I. Sample #, location in section.

II. Name of rock: Grain size: prominent cements, maturity, notable transported constituents, main rock name.

III. Megascopic Description: Structures, color, hardness, rock type.

IV. Microscopic Description:
   A. Texture: Grain size (extreme, 16-84%, mean, where grain size analysis made), distribution, shape.
   B. Authigenic Cements: Kind, distribution, percentage (of rock), paragenic relationships.
   C. Mineral Composition: (type, percentage of terrigenous material, properties of each)
      1. Quartz:
      2. Feldspar:
      3. Miscellaneous terrigenous material:
   D. Remarks.

#971

I. A-4-a, sampled from float, sectioned perpendicular to bedding.

II. Argillaceous, dolomitic microsparite.

III. Very thin-bedded, cross-bedded, medium gray, argillaceous limestone.

IV. A. Grain size: (terrigenous grains) extreme, 4.5 Ø to clay size; 16-84%, 5.20-7.40 Ø; mean, 6.13 Ø. Poorly sorted, fine-skewed, bimodal distribution. Grains are angular.

B. Recrystallization has been extreme. Bedding is shown only by gray streaks of mud. Angular silt, showing replacement by calcite is scattered throughout the rock. X-ray study shows that carbonate is mainly calcite with minor dolomite, total carbonate is 60%.

C. Authigenic pyrite present in abundance. Most has been altered to hematite.

#974

I. A-7-a, sampled 3 feet above base of outcrop.

II. Dolomitic, immature, orthoquartzite mudstone.

III. Blocky, red shale, green reduction spots.

IV. A. Grain size: 4.0 Ø to clay size, intraclasts 2.0 Ø to 3.0 Ø. Poorly sorted. The grains are angular to subround.

B. Dolomite: mainly micrite, intimately mixed with clay matrix, trace silt-sized anhedra. Total less than 20%.

C. 1. Quartz: slightly to strongly undulose extinction, minor composite grains. Most grains contain vacuoles, some clear.

2. Feldspar: plagioclase, trace of orthoclase and microcline, most fresh to slightly altered, some highly vacuolized. Total less than 2%.

3. Metamorphic rock fragments: quartzite,

quartz-mica schist, and mica schist. Total trace.

Clay intraclasts: rounded to elongate, some have micritic dolomite, larger than silt grains. Total trace.

D. Slide heavily iron-stained. Silt grains show coating of clay. Green reduction spots show silt floating in a randomly oriented network of clay. Thicker patches of clay show heavier iron-staining. No evidence of bedding.

#972

I. A-13-e-1, sampled 10 feet above base of outcrop, sectioned perpendicular to bedding.

II. Medium siltstone: calcitic, immature, feldspathic, barite-bearing subgraywacke.

III. Thin-bedded, light gray to tan, resistant siltstone.

IV. A. Grain size: extreme, 1.5 Ø to clay size; 16-84%, 4.03-8.55 Ø; mean, 5.63 Ø. Very poorly sorted, fine-skewed, multi-modal distribution. The grains are angular to round.

B. Calcite: poikilitic development over entire slide, minor replacement of quartz. Total 25-30%.

C. 1. Quartz: straight to strongly undulose extinction, some composite. Many of the fine-sand grains are more angular than the medium and coarse silt. Most grains have vacuoles or microlites, some clear, trace of apatite, zircon, and tourmaline inclusions.

2. Feldspar: plagioclase, minor orthoclase, trace of microcline. Most grains fresh, minor amount of alteration and vacuolization. Total less than 5%.

3. Metamorphic rock fragments: quartzite, quartz-muscovite schist, quartz-chlorite schist, most grains round to subround. Total 5-10%.

Barite: round, radial structure around

silt or indeterminate center, pinkish-orange. Most grains 1.5-2.5 Ø. Total trace.

Carbonate-clay intraclasts: rounded. Total trace.

D. No trace of bedding over entire slide. Thin coating of clay around silt grains. Small patches of very fine silt and clay matrix and floating character of the grains indicate that the carbonate has replaced the original pellitic matrix.

#970

I. A-15-b, lens of Duncan-type siltstone in upper portion of Hennessey Shale, sampled 7.5 feet below base of Duncan.

II. Coarse siltstone: calcitic, dolomitic, immature, intraclast-bearing, feldspathic, MRF-bearing, orthoquartzite.

III. Thick-bedded, medium gray, very resistant siltstone.

IV. A. Grain size: extreme, 1.75 Ø to clay size; 16-84%, 4.10-6.05 Ø; mean, 4.85 Ø. Poorly sorted, fine-skewed, trimodal distribution. The grains are angular to subround.

B. 1. Calcite: poikilitic over entire slide. Replacement of quartz and feldspar is abundant. Total carbonate cement 25-30%.

2. Dolomite: minor, rhombohedral crystals replacing poikilitic calcite.

C. 1. Quartz: straight to strongly undulatory extinction, trace composite, most slightly undulatory. Most grains have vacuoles or microlites, some clear, trace of acicular mineral and biotite inclusions.

2. Feldspar: plagioclase, orthoclase, trace microcline. Orthoclase is fresh to highly vacuolized, plagioclase fresh to moderately altered. Total less than 5%.

3. Metamorphic rock fragments: quartzite and

quartz-mica schist. Smaller and more rounded than quartz and feldspar. Total less than 5%.
Carbonate-clay intraclasts: rounded claystone fragments of carbonate and carbonate-clay. Total less than 5%.

D. No evidence of bedding. Quartz grains are floating in poikilitic cement. Trace of original clay and very fine silt matrix. Stained in places by green and red minerals (malachite and cuprite?), trace only.

#977

I. A-22-a, sampled 1.2 feet below Duncan Sandstone.

II. Dolomitic, immature, calcarenitic orthquartzite mudstone.

III. Blocky, greenish-gray mudstone.

IV. A. Grain size: 3.5 Ø to clay size. Poorly sorted. The grains are angular to subangular.

B. Dolomite: mostly microgranular cement, some silt-sized anhedra and trace of rhombs. Minor replacement of quartz and feldspar. Total less than 25%.

C. 1. Quartz: straight to strongly undulatory extinction, most slightly undulatory, trace stretched composite grains. Most grains have clay coating.

2. Feldspar: plagioclase, orthoclase, trace of microcline, orthoclase highly vacuolized, microcline largely fresh, plagioclase partially altered. Total less than 2%.

3. Metamorphic rock fragments: quartzite and quartz-mica schist. Total trace.
Carbonate and carbonate-clay intraclasts: angular to round, no orientation, primarily carbonate.

D. Dolomite cement quite patchy, possibly due to weathering. No evidence of bedding, some possible burrowing.

#973

I. B-4-a-2, sampled 4 feet above base of outcrop.

II. Dolomitic, immature, intraclast-, feldspar-, and MRF-bearing, orthoquartzite mudstone.

III. Blocky, red shale, green reduction spots.

IV. A. Grain size: 3.75 Ø to clay size. Poorly sorted. The grains are mostly angular, some subround.

B. Dolomite: predominately silt-sized anhedra and rhombs, fairly uniform distribution. Total less than 15%.

C. 1. Quartz: slight to strongly undulose extinction, trace composite grains, most slightly undulatory. Most grains have vacuoles, trace clear and microlites.

2. Feldspar: plagioclase, microcline, trace orthoclase, most fresh to slightly altered, few very fine sand and coarse silt grains of microcline highly altered. Total less than 5%.

3. Metamorphic rock fragments: quartzite, quartz-mica and mica schists. Most smaller than quartz but some coarse silt grains, subangular to round. Total less than 5%.
Clay intraclasts: angular to round, medium sand to fine silt, normally more iron-stained than matrix. Total less than 5%.

D. Slide shows minute cross-bedding with fine lamination, alternating laminae composed of silt and clay. Orientation of mica hash is good. Bedding disrupted, possibly by burrowing. Green reduction spots show only removal of iron-staining. The grains are coated with clay.

#965

I. B-10-b-2, sampled 3.3 feet above base of outcrop.

II. Calcitic, dolomitic, intraclast-bearing, illite-chlorite clay-shale.

III. Slightly fissle green claystone.

IV. A. Grain size: 4.25 Ø to clay size. Poorly sorted. The grains are angular to subround.

B. Carbonate: Few recognizable rhombs of dolomite. Most carbonate in discrete, indistinguishable layers. X-ray studies show it to be predominately calcite, minor dolomite. Total less than 50%.

C. 1. Quartz: straight to strongly undulose extinction, mostly slightly undulose. Most grains contain vacuoles.

2. Feldspar: microcline, plagioclase, orthoclase, most fresh to slightly altered, few coarse silt grains of orthoclase highly vacuolized. Total less than 2%.

3. Metamorphic rock fragments: Quartzite and quartz-mica schist. Total trace.
Clay intraclasts: round to elongate intraclasts, may contain finely divided carbonate, 2.75 Ø to 4.5 Ø. Total less than 5%.

D. This rock is almost a limestone, it is composed of alternating layers of clay and coarse carbonate. Coarse silt grains are scattered uniformly over the slide but finer grains tend to be concentrated in the clay layers. The layers are irregular and discontinuous.

#964

I. C-3-b, Bed "Y", 24.8 feet above base of outcrop, sectioned perpendicular to bedding.

II. Coarse siltstone: dolomitic, quartz-overgrowth cemented, immature, feldspathic, calcarenitic orthoquartzite.

III. Thin-bedded, light gray-green siltstone.

IV. A. Grain size: extreme 3.5 Ø to clay size; 16-84%, 4.30 to 5.8 Ø; mean, 4.94 Ø. Poorly-sorted, fine-skewed, slightly trimodal distribution. The grains are angular to subangular.

B. 1. Dolomite: two types - minute granular coating between grains, silt-sized anhedra and well-shaped rhombs replacing matrix. Some

replacement of quartz and feldspar. Total less than 20%.

2. Quartz-overgrowths: moderately developed but minor amount of cement, form interlocking mosaic, no euhedral faces.

C. 1. Quartz: Straight to strongly undulatory extinction, minor composite grains, most slightly undulatory. Many grains have vacuoles, some have microlites.

2. Feldspar: orthoclase, plagioclase, trace of microcline. Unaltered, angular to subangular, trace of partially altered, rounded plagioclase. Total less than 5%.

3. Metamorphic rock fragments: stretched composite quartz, chlorite and muscovite schists, and quartz-mica schists. Subangular to subround, smaller than average quartz grains. Total less than 2%.
Micas: abundant muscovite, moderate chlorite, trace biotite.
Carbonate Intraclasts: elongate, carbonate and carbonate-clay mud flakes, microgranular.

D. There is evidence of bedding in the form of minor alignment of mica hash, crude alignment of many of the carbonate intraclasts, and silty zones. Most, however, are disrupted.

#978

I. C-6-d-3, sampled 5 feet below top of outcrop.

II. Medium sandstone: dolomitic, submature perthite arenite.

III. Channel filling, light green, very friable argillaceous sandstone.

IV. A. Grain size: 2mm to clay size, mean 2.0 Ø. Poorly sorted. The grains are angular to subround.

B. Dolomite: silt to sand-sized anhedra as well as microgranular cement, some anhedra contain clay. Some replacement of feldspar and trace of replacement of quartz. Total 15%.

C. 1. Quartz: most straight to slightly undulatory, some strongly undulatory, patchy extinction. Many grains have trails of vacuoles (fractures), few microlites, trace-zircon and apatite inclusions. 40%.

2. Feldspar: perthite, some antiperthite, trace of plagioclase, partially altered to highly vacuolized. Some microcline recognizable in perthite. 60%.

3. Approximately ¼ of clastic grains are perthite granite fragments, trace of myrmkite.

D. In most cases the grains are separated from the coarse carbonate by a thin layer of clay and finely divided carbonate. The mineralogy of this slide is different from the bulk of the other material in that the clastic fragments are obviously derived from the Wichita Mountains.

#966

I. C-9-c, Bed "W", sampled 19.5 feet above base of the outcrop, sectioned perpendicular to bedding.

II. Medium siltstone: dolomitic, immature, feldspathic orthoquartzite.

III. Very thin-bedded, light gray-green, slightly friable siltstone.

IV. A. Grain size: extreme, 0.5 Ø to clay size; 16-84%, 4.28-6.45 Ø; mean, 5.11 Ø. Poorly sorted, fine-skewed, trimodal distribution. The grains are angular to subround.

B. Dolomite: microgranular cement, trace of silt-sized anhedra and rhombs, moderate replacement of quartz. Total 20%.

C. 1. Quartz: straight to strongly undulatory extinction, mostly slightly undulatory.

2. Feldspar: orthoclase, plagioclase, trace microcline. Most orthoclase and plagioclase moderately to highly altered, microcline smaller and fresher. One grain, combined perthite and Carlsbad twin,

present in slide, medium sand, slightly altered, angular. Total less than 5%.

3. Metamorphic rock fragments: quartzite and quartz-mica schist. Total trace.

D. Lamination good but disrupted. Some orientation of mica, pronounced concentration of silt in laminae, carbonate mud streaks, some cross-bedding.

#967

I. C-9-f, Bed "X", sampled 52 feet above base of the outcrop, sectioned perpendicular to bedding.

II. Coarse siltstone: dolomitic, immature subarkose.

III. Very thin-bedded, light tannish-gray siltstone.

IV. A. Grain size: extreme, 3.0 Ø to clay size; 16-84%, 4.20-5.70 Ø; mean, 4.80 Ø. Poorly sorted, fine-skewed, trimodal distribution. The grains are angular to subround.

B. Dolomite: microgranular cement, minor amount of silt-sized rhombs and anhedra, minor replacement of quartz. Total 20%.

C. 1. Quartz: Straight to strongly undulatory, trace of composite grains, mostly slightly undulatory extinction. Many grains have thin clay coating. Most are clear, few have vacuoles or microlites, trace of zircon inclusions.

2. Feldspar: orthoclase, plagioclase, minor microcline, orthoclase more altered than plagioclase, microcline mostly fresh, large grains more altered than small. Total 5-10%.

3. Metamorphic rock fragments: quartzite and quartz-mica schists. Total trace.

D. Evidence of bedding is moderate: alignment of micas, concentration of silt in some laminae, mud and carbonate in others. Some cross-bedding evident, much disruption of bedding.

#968

I. C-9-j, Bed "Y", sampled 69.3 feet above base of outcrop, sectioned perpendicular to bedding.

II. Coarse siltstone: dolomitic, quartz- and feldspar-overgrowth cemented, immature, calcarenitic, feldspathic orthoquartzite.

III. Thin-bedded, ripple-marked, light gray siltstone.

IV. A. Grain size: extreme 3.0 Ø to clay size; 16-84%, 4.25-5.10 Ø; mean 4.60 Ø. Poorly sorted, fine-skewed, trimodal distribution. The grains are angular to subangular.

B. 1. Dolomite: both granular, micritic dolomite and silt-size anhedra and rhombs. Total 20%. Some replacement of quartz and feldspar by dolomite.

2. Quartz-overgrowths: faint, small portion of the cement, commonly enclose minute carbonate crystals along grain boundaries, clear, no growth stages.

3. Feldspar-overgrowths: very faint, trace.

C. 1. Quartz: straight to strongly undulatory extinction, some composite grains, most slightly undulatory. Some grains have vacuoles and some have microlites.

2. Feldspar: plagioclase and orthoclase. Angular to subangular, most fresh, some altered, trace highly altered. Total less than 5%.

3. Metamorphic rock fragments: quartz-chlorite schist, mica schist, trace quartzite. Smaller than quartz grains. Total less than 2%.
Carbonate intraclasts: round carbonate balls and some elongate carbonate-clay flakes.

D. Lamination is prominent - some alignment of mica hash; placer concentrations of magnetite, leucoxene, and hematite; concentration of intraclasts and silt in separate layers. Burrowing is obvious but minor.

#969

I. C-9-m, Bed "Zb", sampled 85.3 feet above base of outcrop, sectioned perpendicular to bedding.

II. Medium siltstone: dolomitic, immature orthoquartzite.

III. Very thin to thin-bedded, light gray siltstone.

IV. A. Grain size: extreme, 3.25 Ø to clay size: 16-84%, 4.55-6.67 Ø; mean, 5.48 Ø. Poorly sorted, fine-skewed, bimodal distribution. The grains are angular to subround.

B. 1. Dolomite: microgranular cement and silt-sized rhombs and anhedra. Some replacement of quartz. Total 25%.

2. Quartz-overgrowths: vague, trace present, carbonate inclusions along grain boundary.

C. 1. Quartz: most slightly to strongly undulatory, trace straight extinction and composite grains. Some grains have thin clay coating. Most have vacuoles, few clear.

2. Feldspar: plagioclase, trace of orthoclase and microcline, most fresh, largest grains more altered than smallest, orthoclase more altered than plagioclase. Total less than 2%.

3. Metamorphic rock fragments: quartz-chlorite schist, quartzite. Smaller and more rounded than quartz. Total less than 2%.

D. Evidence of bedding scarce, limited to poor alignment of mica flakes and traces of carbonate and clay mud flakes in crude alignment. Silt not concentrated in laminae.

I. C.H. A1-1-6, sampled 109 feet above base of core, sectioned parallel to bedding.

II. Coarse siltstone: dolomitic, immature, intraclast-bearing orthoquartzite.

III. Thinly laminated, green, slightly friable siltstone.

IV. A. Grain size: 3.5 Ø to clay size; intraclasts 1.0-4.5 Ø. Poorly sorted. The grains are angular to subround.

B. 1. Dolomite: mostly euhedral rhombs and some anhedra from 4 to 8 Ø. Minor replacement of quartz. Total less than 15%.

2. Quartz-overgrowths: trace, faint, no growth stages. Some have carbonate inclusions.

C. 1. Quartz: straight to strongly undulatory extinction, mostly slightly undulatory, trace composite. Most grains have vacuoles, few clear. Trace of sericitization.

2. Feldspar: orthoclase, plagioclase, microcline. Mostly fresh, a few grains slightly altered. Total trace.

3. Metamorphic rock fragments: quartzite, quartz-chlorite schist. Total trace.
Intraclasts: mainly rectangular and polygonal with trace of rounded areas, composed of oriented clay. Trace of silt and only minor carbonate.

D. Silt is concentrated between intraclasts. Some fractures in intraclasts, possibly dessication cracks. The silt grains are clay coated.

I. C.H. A1-2-5, sampled 136 feet above base of core.

II. Argillaceous, very finely crystalline, intraclastic, feldspathic dolomite.

III. Blocky, soft, red shale.

IV. A. Grain size: (terrigenous grains) 3.75 Ø to clay size, (intraclasts) 1.5-4.5 Ø. Poorly sorted. The grains are angular to subround.

B. Carbonate extensively recrystallized. Intraclasts identified by higher concentration of iron-staining, lower silt content, and microgranular texture. Intraclasts angular to round, somewhat flattened. Minor replacement of quartz.

C. 1. Quartz: straight to strongly undulose

extinction, mostly slightly undulose. Most grains have vacuoles or microlites, few clear.

2. Feldspar: plagioclase, orthoclase, trace microcline, most grains fresh, some slightly altered. Total less than 5%.

3. Metamorphic rock fragments: quartzite and quartz-mica schist. Total less than 2%.

D. This rock was probably composed of carbonate intraclasts in a matrix of silt, clay, and micrite. Iron-staining is present but the matrix is noticeably less stained than the intraclasts. Burrowing is probably indicated as large areas are uniformly mixed. Recrystallization is extreme.

I. C.H. A1-2-13, sampled 65.5 feet above base of core, sectioned perpendicular to bedding.

II. Dolomitic, gypsiferous, immature orthoquartzite mudstone.

III. Laminated, light and medium green shale.

IV. A. Grain size: 4.5 Ø to clay size; mean, fine silt. Poorly sorted. The grains are angular to subangular.

B. 1. Dolomite: silt-sized anhedra and rhombs, uniform distribution throughout slide. Total less than 15%.

2. Gypsum: mostly large-scale satin spar replacement areas, minor gypsum fibers throughout matrix. Minor.

C. 1. Quartz: slightly to strongly undulatory extinction, trace composite grains. Most clear, some with vacuoles.

2. Feldspar: plagioclase, some orthoclase, most fresh. Total trace.

D. Lamination in the hand specimen is prominent but minor in thin section. A few streaks of opaque material and silt are present. Good orientation of mica flakes.